Developmental Biology 356 (2011) 460–474

Contents lists available at ScienceDirect

Developmental Biology

journal homepage: www.elsevier.com/developmentalbiology

Involvement of multimeric protein complexes in mediating the capacitation-dependent binding of human spermatozoa to homologous zonae pellucidae☆

Kate A. Redgrove [a], Amanda L. Anderson [a], Matthew D. Dun [a], Eileen A. McLaughlin [a,b], Moira K. O'Bryan [c], R. John Aitken [a,b], Brett Nixon [a,*]

[a] Reproductive Science Group, School of Environmental and Life Sciences, Discipline of Biological Sciences, University of Newcastle, Callaghan, NSW 2308, Australia
[b] ARC Centre of Excellence in Biotechnology and Development, School of Environmental and Life Sciences, University of Newcastle, Callaghan, NSW 2308, Australia
[c] School of Biological Sciences, The Department of Anatomy and Development Biology, Monash University, Melbourne, VIC 3800, Australia

ARTICLE INFO

Article history:
Received for publication 5 October 2010
Revised 31 May 2011
Accepted 31 May 2011
Available online 13 June 2011

Keywords:
Spermatozoa
Fertilization
Capacitation
Proteasome

ABSTRACT

The recognition and binding of a free-swimming spermatozoon to an ovulated oocyte is one of the most important cellular interactions in biology. While traditionally viewed as a simple lock and key mechanism, emerging evidence suggests that this event may require the concerted action of several sperm proteins. In this study we examine the hypothesis that the activity of such proteins may be coordinated by their assembly into multimeric recognition complexes on the sperm surface. Through the novel application of blue native polyacrylamide gel electrophoresis (BN-PAGE), we tender the first direct evidence that human spermatozoa do indeed express a number of high molecular weight protein complexes on their surface. Furthermore, we demonstrate that a subset of these complexes displays affinity for homologous zonae pellucidae. Proteomic analysis of two such complexes using electrospray ionization mass spectrometry identified several of the components of the multimeric 20S proteasome and chaperonin-containing TCP-1 (CCT) complexes. The latter complex was also shown to harbor at least one putative zona pellucida binding protein, ZPBP2. Consistent with a role in the mediation of sperm–zona pellucida interaction we demonstrated that antibodies directed against individual subunits of these complexes were able to inhibit sperm binding to zona-intact oocytes. Similarly, these results were able to be recapitulated using native sperm lysates, the zona affinity of which was dramatically reduced by antibody labeling of the complex receptors, or in the case of the 20S proteasome the ubiquitinated zonae ligands. Overall, the strategies employed in this study have provided novel, causal insights into the molecular mechanisms that govern sperm–egg interaction.

Introduction

Fertilization is a major biological process involving a complex interplay of cellular interactions between the male and female gametes. In mammals, this process is initiated by a cell- and species-specific binding event that occurs between free-swimming spermatozoa and the zona pellucida (ZP), a protective glycoprotein matrix that surrounds the ovulated oocyte. Although numerous ZP receptors have been implicated in the process, failure of the corresponding knockouts to deliver the anticipated infertility phenotype has encouraged revision of the traditional view that this interaction can be attributed to a single, constitutively expressed, sperm receptor molecule (Cho et al., 1998; Ensslin and Shur, 2003; Lu and Shur, 1997; Nishimura et al., 2001; Shamsadin et al., 1999). Instead of this simple lock and key mechanism, an alternative hypothesis has been advanced suggesting that spermatozoa employ a suite of multimolecular protein complexes to coordinate their adhesion to ligands presented by homologous zonae pellucidae (Asquith et al., 2004; Gadella, 2008; Nixon et al., 2007). Such a model is analogous to the dynamic, tightly regulated processes that drive many somatic cell–matrix and cell–cell interactions (Ebnet, 2008; Shen et al., 2008; Shotton et al., 1979; Takakuwa et al., 1986).

Another important attribute of sperm–ZP interaction is that spermatozoa do not achieve the ability to engage in this process until they have completed their post-testicular maturation. Since spermatozoa are transcriptionally silent (Ward and Zalensky, 1996), such maturation relies heavily on post-translational modifications driven by changes in the microenvironment to which these cells are exposed on their journey from the testes to the surface of the oocyte (Cooper, 1986). The first of these microenvironments is the epididymis. As spermatozoa

☆ Grant support: National Health and Medical Research Council of Australia (NHMRC 569235) and Hunter Medical Research Institute (HMRI 08-15).

* Corresponding author at: School of Environmental and Life Sciences, Discipline of Biological Sciences, University of Newcastle, University Drive, Callaghan, NSW 2308, Australia. Fax: + 61 2 4921 6308.
E-mail address: Brett.Nixon@newcastle.edu.au (B. Nixon).

0012-1606/$ – see front matter © 2011 Elsevier Inc. All rights reserved.
doi:10.1016/j.ydbio.2011.05.674

are conveyed through this organ they undergo a remodeling process that includes dramatic alterations in the lipid and protein architecture of the plasma membrane (Aveldano et al., 1992; Jones, 1989; Jones, 1998; Olson and Hinton, 1985; Syntin et al., 1996), culminating in acquisition of the potential for forward progressive motility and a capacity to bind to the ZP (for reviews see Cooper, 1986; Cornwall, 2009). However, the expression of this functional potential is not realized until completion of the final maturation phase, termed 'capacitation', which occurs as spermatozoa ascend the female reproductive tract (Austin, 1951; Chang, 1951). Since only capacitated cells can bind to the ZP it follows that any attempt to unravel the molecular basis of this binding process is predicated on a thorough understanding of the key changes that drive spermatozoa into a state of capacitation.

Unfortunately, capacitation has proven to be an inordinately complex process incorporating a number of species-specific phenomena. Recent advances have revealed that in human spermatozoa, capacitation may be initiated by engagement of surface receptors (Nixon et al., 2006) and the subsequent induction of complex signaling pathways that ultimately converge to promote an impressive up-regulation of tyrosine phosphorylation across myriad target proteins (Leclerc et al., 1996, 1998; Lefievre et al., 2002; Mitchell et al., 2008; Visconti et al., 1995a, 1995b). While the precise mechanisms remain to be unequivocally established, these biochemical changes appear causally linked to the surface remodeling events that allow spermatozoa to adhere to the ZP (Cross, 2003; Gadella et al., 2008; Harrison et al., 1996; Harrison and Gadella, 2005; Myles and Primakoff, 1984; Yanagimachi, 1994).

In this study we have examined the hypothesis that capacitation leads to either the assembly and/or functional activation of multimeric protein complexes responsible for mediating sperm–ZP interaction. To facilitate these studies we have employed blue native polyacrylamide gel electrophoresis (BN-PAGE), an electrophoretic technique originally developed for the analysis of mitochondria (Nijtmans et al., 2002; Schagger and von Jagow, 1991; Wittig et al., 2006), to isolate intact, biologically active protein complexes from human spermatozoa. Although this technique has been widely embraced as a method for isolating membrane bound protein complexes in cells from species as diverse as plants, algae and bacteria (Eubel et al., 2005; Heuberger et al., 2002; Katz et al., 2007; Kjell et al., 2004), this is the first report of BN-PAGE being used for the analysis of human spermatozoa. The results provide novel, compelling evidence that the binding of human spermatozoa to the ZP is orchestrated by multimeric protein complexes.

Materials and methods

Reagents

Unless specified, chemical reagents were obtained from Sigma (St. Louis, MO) and were of research grade. The following primary antibodies were purchased to characterize proteins of interest: anti-20S proteasome alpha-subunit and anti-20S proteasome beta-subunit sampler packs (Enzo Life Sciences International, Inc., Plymouth, PA), anti-CCT8 (Santa Cruz Biotechnology, Santa Cruz, CA), anti-CCT6A (Santa Cruz Biotechnology), anti-CCT2 (Genwaybio, San Diego, CA), anti-CCT3 (Proteintech Group Inc, Chicago, IL), and anti-ZPBP2 (Abnova, Taipei City, Taiwan). Anti-phosphotyrosine monoclonal antibody (clone 4G10) was from Upstate Biotechnology (Lake Placid, NY). Anti-ubiquitin antibodies were from Abcam (Cambridge, MA). Goat anti-rabbit IgG conjugated fluorescein isothiocyanate (FITC) and rabbit anti-goat IgG FITC secondary antibodies were purchased from Sigma. Horseradish peroxidase (HRP) conjugated streptavidin was purchased from Chemicon (Temecula, CA). Tetramethyl rhodamine isothiocyanate (TRITC) conjugated lectin from *Arachis hypogaea* (PNA) was from Sigma. The SYTOX green cell vitality stain was purchased from Invitrogen (Carlsbad, CA). Nitrocellulose was from Amersham (Buckinghamshire, UK). Highly pure Coomassie brilliant blue G250 was from Serva (Heidelberg, Germany).

Preparation of human spermatozoa

The experiments described in this study were conducted with human semen samples obtained from a panel of healthy normozoospermic donors, in accordance with the Institutes' Human Ethics Committee guidelines. These samples were collected *via* masturbation into sterile specimen containers after an abstinence period of 48 h and delivered to the laboratory within 1 h of ejaculation. Purification of human spermatozoa from these samples was achieved using a 44% and 88% discontinuous Percoll (GE Healthcare, Piscataway, NJ) gradient as described previously (Nixon et al., 2005). Purified spermatozoa were recovered from the base of the 88% Percoll fraction and resuspended in Biggers, Whitten and Whittingham medium (BWW; Biggers et al., 1971), composed of 91.5 mM NaCl, 4.6 mM KCl, 1.7 mM $CaCl_2.2H_2O$, 1.2 mM KH_2PO_4, 1.2 mM $MgSO_4.7H_2O$, 25 mM $NaHCO_3$, 5.6 mM D-glucose, 0.27 mM sodium pyruvate, 44 mM sodium lactate, 5 U/ml penicillin, 5 mg/ml streptomycin, 20 mM HEPES buffer and 1 mg/ml polyvinyl alcohol (PVA) (osmolarity of 300 mOsm/kg). The cells were then pelleted by centrifugation at 500 *g* for a further 15 min and resuspended at a concentration of 10×10^6 cells/ml before being assessed for cell motility and vitality. The latter was examined by staining spermatozoa with SYTOX Green (0.5 μM for 15 min), a high-affinity, fluorescent nucleic acid stain that is impermeant to live cells and thus an indicator of cell viability. Samples in which either parameter was below 85% were discarded.

Preparation of human oocytes

Human oocytes were obtained with informed consent from patients of the Hunter IVF Clinic. These oocytes were either immature or had failed to be fertilized following intracytoplasmic sperm injection. Prior to use the oocytes were fixed in a high salt medium consisting of 1.5 M $MgCl_2$, 0.1% dextran, 0.01 mM HEPES buffer and 0.1% PVA and stored at 4 °C. Notwithstanding degeneration of the oocyte, this form of storage has been demonstrated to retain the biological characteristics of the zona pellucida (Yanagimachi et al., 1979).

Capacitation of human spermatozoa

Following dilution in BWW, purified spermatozoa were incubated at 37 °C under an atmosphere of 5% CO_2:95% air. Non-capacitated cells were incubated in BWW prepared without $NaHCO_3$ (BWW-HCO_3^-) but with additional NaCl incorporated to maintain an osmolarity of 300 mOsm/kg. The formation of bicarbonate in these samples was prevented by capping the tubes throughout the incubation. Capacitated cells were incubated in BWW supplemented with 3 mM pentoxifylline (ptx) and 5 mM dibutyryl cyclic adenosine monophosphate (dbcAMP). Incubations were conducted for a period of 3 h with gentle mixing at regular intervals to prevent settling of the cells. At the end of the incubation an aliquot of each sperm suspension was removed and assessed for cell motility and vitality. Importantly, neither parameter was adversely affected by any of the treatments used in this study (*i.e.* remained above 85%). The remainder of the sperm sample was prepared for the various treatments outlined below. The capacitation conditions used have been shown to induce optimal capacitation as defined by tyrosine phosphorylation, hyperactivation and, critically, zona binding (Mitchell et al., 2007; Mitchell et al., 2008). These conditions also yield similar levels of capacitation to those obtained using a standard human *in vitro* fertilization system (Sydney IVF Sperm Medium, K-SISM, Cook Medical, Brisbane, Australia) (Fig. 1; Nixon et al., in press).

Biotinylation of sperm surface proteins

In order to examine the surface orientation of native protein complexes, spermatozoa were labeled with sulfo-NHS-LC-biotin (Pierce, Rockford, IL), a membrane impermeable derivative of biotin, in accordance with the manufacturer's instructions. For this purpose,

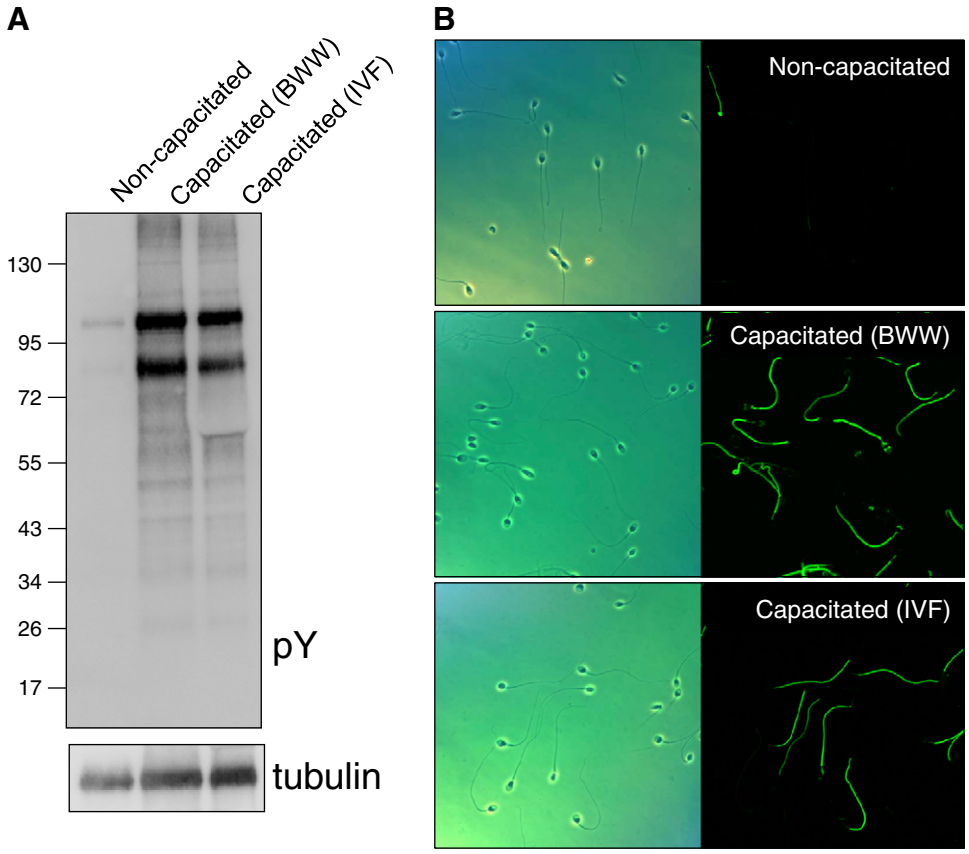

Fig. 1. Comparison of the levels of capacitation achieved in modified BWW media and that of standard IVF media. Populations of non-capacitated and capacitated human spermatozoa were prepared in BWW lacking $NaHCO_3$ (non-capacitated), BWW supplemented with ptx and dbcAMP (capacitated BWW) or IVF media (capacitated IVF). The cells were then prepared for assessment of their phosphotyrosine status using (A) immunoblotting and (B) immunocytochemistry. Both systems used for induction of sperm capacitation yielded high levels of phosphotyrosine expression that were virtually indistinguishable (note that the diffuse band of approximately 60 kDa that appears in the capacitated IVF lane of the immunoblot corresponds to the presence of human serum albumin in the IVF media used to prepare this sample).

spermatozoa were incubated in the presence of 0.5 mg/ml sulfo-NHS-LC-biotin during the final 30 min of capacitation (Nixon et al., 2005). Following the completion of capacitation, the biotinylation reaction was quenched through the addition Tris–HCl (pH 7.4) to a final concentration of 1 mM. The cells were then washed 3× in BWW prior to protein extraction. Importantly, the biotinylation reaction had no discernible effect upon cell motility, vitality or the efficacy of the capacitation process. The latter was assessed by the level of phosphotyrosine expression observed in biotinylated cells, which appeared indistinguishable to that seen in untreated samples (data not shown).

Immunolocalization on fixed spermatozoa

Following incubation, spermatozoa were fixed in 4% paraformaldehyde, washed three times with 0.05 M glycine in phosphate-buffered saline (PBS), plated onto poly-L-lysine coated glass slides and air-dried. All subsequent incubations were performed in a humid chamber at 37 °C. The cells were blocked with 10% serum/3% BSA for 1 h. Slides were washed 3× with PBS for 5 min and incubated in a 1:100 dilution of primary antibody at 4 °C overnight. Slides were then subjected to 3×5 min washes with PBS and incubated in a 1:100 dilution of an appropriate FITC-conjugated secondary antibody (1:300 for anti-mouse FITC) for 1 h at 37 °C. Slides were again washed and mounted in 10% mowiol 4-88 (Calbiochem) with 30% glycerol in 0.2 M Tris (pH 8.5) with 2.5% 1,4-diazobicyclo-(2.2.2)-octane (DABCO). Cells were examined using either a Zeiss Axioplan 2 fluorescence microscope or a Zeiss LSM510 laser scanning confocal microscope equipped with argon and helium/neon lasers (Carl Zeiss, Thornwood, NY).

Blue native polyacrylamide gel electrophoresis

Following incubation under either capacitating or non-capacitating conditions, suspensions of 1×10^8 sperm/ml were lightly pelleted (300 *g* for 5 min) and resuspended in native protein lysis buffer consisting of: 1% n-dodecyl β-D-maltoside which was adjusted to a final concentration below that of the critical micellar concentration, 0.5% Coomassie Blue G250 and a cocktail of protease inhibitors (Roche, Mannheim, Germany). The samples were gently mixed and then incubated at 4 °C on an orbital rotator for 30 min. Following incubation, the lysate was recovered by centrifugation at 14,000 *g* for 20 min at 4 °C and dialyzed against the Blue native cathode buffer (Invitrogen), to remove any excess salts and detergents. Following dialysis, the sample was placed in a clean 1.5 ml tube and glycerol was added to a final concentration of 5% (v/v).

For the purpose of one dimensional blue native page (1D BN-PAGE), native protein lysates were loaded onto pre-cast blue native polyacrylamide gels (NativePAGE Novex 4–16%, Bis–Tris; Invitrogen) and resolved using the NativePAGE cathode and anode buffer system (Invitrogen). This system is based in the BN-PAGE technique originally developed by Schagger et al.(1994) and Schagger and von Jagow(1991) and optimized for use in spermatozoa (M. Dun, personal communication). The BN-PAGE electrophoresis apparatus was placed at 4 °C and the samples were separated at 100 V until the Coomassie dye front reached the bottom of the loading wells. The voltage was then increased to 200 V and the separation continued until the Coomassie dye front reached the bottom of the gel. The gels were then removed from the electrophoresis apparatus and stained sequentially with Coomassie G250 then silver stained (to detect less abundant proteins). Alternatively, the gels were

prepared for either Western blotting or two dimensional BN-PAGE (2D BN-PAGE).

2D BN-PAGE was conducted in order to resolve native protein complexes into their individual components. For this purpose, individual lanes of the 1D BN-PAGE gel were excised and then pre-equilibrated in SDS-PAGE sample buffer (2% w/v SDS, 10% w/v sucrose in 0.1875 M Tris, pH 6.8) supplemented with 0.5% v/v dithiothreitol (DTT) and 4% v/v iodoacetamide for 10 min. The lanes were then placed on top of a 10% SDS-PAGE gel prepared without stacking wells and sealed in position using 0.5% molten agarose. The gel was placed in a small-format electrophoresis chamber (Bio-Rad Laboratories, Hercules, CA), immersed in SDS-PAGE running buffer and electrophoresed at 100 V until the Coomassie dye front reached the bottom of the gel. Gels were then removed from their cassettes and either stained with Coomassie G-250 or prepared for Western blotting.

Western and Far Western blotting

Proteins resolved by either 1D or 2D BN-PAGE were transferred onto nitrocellulose membranes using conventional Western blotting techniques (Towbin et al., 1979). In order to detect proteins of interest, membranes were blocked with 3% w/v BSA in Tris-buffered saline (TBS; pH 7.4) supplemented with 0.1% polyoxyethylenesorbitan monolaurate (Tween-20). Membranes were rinsed in TBS and then probed with appropriate primary antibodies (diluted 1:1000 dilution in TBS supplemented with 1% BSA and 0.1% Tween-20) for 2 h at room temperature. Following incubation, membranes were washed 3× in TBS containing 0.1% Tween-20 (TBST) for 10 min. Membranes were then probed for 1 h with an appropriate HRP-conjugated secondary antibody (diluted between 1:3000 and 1:5000 in TBST/1% BSA) at room temperature. Following a further 3 washes in TBST, cross reactive proteins were visualized using an enhanced chemiluminescence kit (GE Healthcare) according to the manufacturer's instructions.

To detect native protein complexes with affinity for zona pellucidae, 1D BN-PAGE gels were transferred to nitrocellulose membranes, blocked with 3% w/v BSA in TBS for 1 h before being prepared for Far-Western blotting with solubilized, biotin-labeled preparations of zona pellucidae. These zonae were prepared by incubation of human oocytes (approximately 100/experiment) in 1 mg/ml sulfo-NHS-LC-biotin at 37 °C for 30 min. The biotin reaction was quenched by the addition of Tris (pH 7.4) to a final concentration of 1 mM. Oocytes were washed 3 times to remove unbound biotin and the zonae pellucidae solubilized by incubation in acidified Hank's buffered salt solution (pH adjusted to 2.0 with 1 M HCl) for 15 min at 37 °C. Solubilized zona proteins were removed from insoluble oocyte material by aspiration with a fine bore micropipette, and then the pH readjusted to 7.4 with 1 M NaOH. This preparation of zona pellucidae was then incubated with the BN-PAGE Western blots overnight at 4 °C on an orbital rotator. Membranes were then washed 3 times in TBST before incubation with HRP-conjugated streptavidin (diluted 1:4000 in 1% w/v BSA/TBST). Labeled complexes were then detected using ECL as described above. This experiment was repeated twice with similar results obtained in each replicate.

Protein identification

The proteins present in native complexes that displayed affinity for homologous zonae pellucidae were further resolved by 2D BN-PAGE. Individual proteins were then carefully excised and sequenced at the Australian Proteome Analysis Facility using an electrospray ionization mass spectrometry interface. In preparation for sequencing, the gel slices were destained then reduced (25 mM DTT in 25 mM ammonium bicarbonate) and alkylated (55 mM iodoacetamide in 25 mM ammonium bicarbonate). The proteins within the gel slice then underwent a 16 h tryptic digest at 37 °C. After digestion, 0.1% trifluoroacetic acid (TFA) was added and the sample sonicated for 10 min.

The resulting digested peptides were separated by nano-liquid chromatography (LC) using a CapLC system (Agilent 1100 Series, Agilent Technologies, Germany). Samples were injected onto a peptide trap (Michrome Peptide Captrap) for pre-concentration and desalted with 0.1% TFA at 10 μl/min. The peptide trap was then switched into line with the analytical column containing C18 reverse phase silica (SGE ProteCol C18, 300A, 3 μm × 150 μm × 10 cm).

Peptides were eluted from the column using a linear solvent gradient, with steps, from H_2O:CH_3CN (95:5 + 0.1% formic acid) to H_2O:CH_3CN (20:80 + 0.1% formic acid) at 500 nl/min over a 130 min period. The LC eluent was subjected to positive ion nanoflow electrospray analysis on an Applied Biosystems QSTAR XL mass spectrometer (ABI, CA). The QSTAR was operated in an information dependent acquisition mode (IDA). In IDA mode a time of flight mass spectrometry (TOFMS) survey scan was acquired (m/z 380–1600, 0.5 s), with the three largest multiply charged ions (counts > 70) in the survey scan sequentially subjected to MS/MS analysis. MS/MS spectra were accumulated for 2 s (m/z 100–1600).

The LC–MS/MS data were searched using Mascot (Matrix Science, London, UK). Mascot was used to search entries for species *Homo sapiens* in the SwissProt protein database with the following search parameters: maximum of one missed trypsin cleavage, cysteine carbamidomethylation, methionine oxidation, and a maximum 0.2-Da error tolerance in both the MS and MS/MS data. High confidence positive identifications were based on a minimum of two matching peptides and were confirmed or qualified by operator inspection of the spectra and search results.

Co-immunoprecipitation

Approximately 60 μl (per treatment) magnetic Protein G-coated Dynabeads (Dynal Biotech ASA, Oslo, Norway) were washed 3× in washing and binding buffer (5 mM Tris–HCl (pH 7.5), 0.5 mM EDTA, 1 M NaCl). This was followed by conjugation with 4 μg anti-CCT6A antibody at 4 °C overnight with constant mixing. A control sample of beads was left non-conjugated and was incubated with washing and binding buffer only. Following conjugation the beads were washed twice in washing and binding buffer. Capacitated spermatozoa were then lyzed in IP lysis buffer [0.1% (v/v) Triton X-100, 300 mM NaCl, 20 mM Tris, pH 7.4 supplemented with protease inhibitor cocktail and a 1:100 dilution of HALT complete phosphatase inhibitor cocktail (Pierce)]. Approximately 100 μg of soluble lysate was added to the pre-adsorbed beads and left to incubate at 4 °C overnight with constant mixing. Following incubation, the beads were washed twice in washing and binding buffer and resuspended in SDS sample buffer. The suspension was then boiled for 5 min, the beads were removed and the precipitated proteins were resolved on 10% polyacrylamide gels before being electro-transferred onto nitrocellulose membranes and immunoblotted as described previously. Control incubations were included where beads were incubated with sperm lysate in the absence of antibody, and also antibody-conjugated beads were incubated in the absence of cell lysate. These controls were processed as described above.

Duolink proximity ligation assay (PLA)

Duolink *in situ* primary ligation assays (PLA) were conducted in accordance with the manufacturer's instructions (OLINK Biosciences, Uppsala, Sweden). Briefly, human spermatozoa were purified and capacitated as previously described, after which time they were fixed in 2% paraformaldehyde and coated onto poly-L-lysine slides overnight at 4 °C. These cells were then incubated in blocking solution (OLINK Biosciences) for 1 h at 37 °C in a humidified chamber, before target proteins were sequentially labeled with a pair of appropriate primary antibodies raised in different species (anti-CCT6A and anti-ZPBP2; or anti-CCT6A and anti-tubulin; or anti-CCT6A alone for a negative control) overnight at 4 °C in a humidified chamber. After washing, appropriate

secondary antibodies (anti-mouse for ZPBP2 and tubulin and anti-goat for CCT6A) conjugated to complementary synthetic oligonucleotides (PLA probes, OLINK Biosciences) were then applied to the samples for 1 h at 37 °C. The samples were then sequentially hybridized (15 min), washed and enzymatically ligated (15 min). If the target proteins reside in close proximity, this reaction leads to the production of a signal that appears as a discrete fluorescent dot. These signals were visualized with an Axio Imager A1 fluorescence microscope (Carl Zeiss Microimaging, Inc, Thornwood, NY) and pictures taken using an Olympus DP70 microscope camera (Olympus America, Center Valley, PA).

Sperm–zona pellucida binding assays

To examine the physiological importance of protein complexes in relation to sperm–zona pellucida interaction, capacitated spermatozoa were prepared and incubated with the appropriate antibodies (diluted 1:100) for 30 min at 37 °C. The spermatozoa were then co-incubated with zona-intact human oocytes for 30 min at 37 °C as previously described (Nixon et al., in press). After stringent washing of the oocytes by repeated aspiration through a fine bore pipette, the number of spermatozoa remaining bound to each zona pellucida was counted using phase contrast microscopy. In separate experiments, native sperm lysates were prepared from 1×10^8 cells and dialyzed overnight against BWW to remove excess detergent. The lysates were then divided among treatment groups and co-incubated in a 20 µl droplet with a minimum of five zona-intact oocytes for 30 min at 37 °C on a shaking platform. The oocytes were stringently washed (as above) prior to being sequentially labeled with appropriate primary and FITC-conjugated secondary antibodies directed against the proteins of interest (Fig. S1). In order to determine the specificity of binding, equivalent amounts of the native sperm lysates were preincubated with antibodies directed against the respective target proteins prior to being exposed to the oocytes (Fig. S1). Fluorescent signals indicating the presence of bound protein complexes were visualized with an Axio Imager A1 fluorescence microscope (Carl Zeiss). This experiment was replicated three times.

Results

Human spermatozoa express a number of surface oriented multimeric protein complexes

The separation of native multimeric protein complexes from populations of human spermatozoa was achieved using BN-PAGE techniques optimized for use with mammalian spermatozoa from the methodologies originally described by Schagger and von Jagow (1991) (Fig. 2). The application of these protocols consistently resolved over 15 predominant protein bands ranging in molecular weight from approximately 70 kDa to >1000 kDa (Fig. 2). Furthermore, this profile of native protein extracts did not display any marked inter- (Fig. 2A) or intra-donor (Fig. 2B) variability. Among the observed protein bands, the majority possessed a high molecular weight (>250 kDa) consistent with the anticipated presence of multimeric entities, rather than individual, high molecular weight proteins. Support for this conclusion was advanced by the application of 2D BN-PAGE to separate the individual constituents of these putative complexes (Fig. 2C). As anticipated, this technique effectively resolved a majority of complexes into a number of discrete proteins (Fig. 2D). In most instances, the combined molecular weights of the individual proteins closely approximated that of the complex in which they resided. Taken together these results demonstrate the utility of the BN-PAGE system for the isolation of intact protein complexes from human spermatozoa.

To investigate the influence of capacitation status on the expression of protein complexes in human spermatozoa, native extracts were prepared from populations of non-capacitated and capacitated cells (Fig. 3). Notwithstanding qualitative similarities in the BN-PAGE profile of proteins isolated from both sperm populations, changes in the relative abundance of several complexes were observed following the capacitation of these cells (Fig. 3A). For this analysis, protein quantification was extremely difficult because BN-PAGE necessitates protein staining with Serva blue dye during lysis, negating the use of traditional protein quantification methods. Instead, the number of capacitated and non-capacitated spermatozoa extracted for analysis was carefully standardized. The fact that many of the proteins bands greater than 720 kDa appeared to display similar levels of staining intensity in both samples (Fig. 3A) suggests that this strategy was reasonably successful. However, a number of the protein bands that resolved below 720 kDa appeared to be stained more intensely in samples recovered from capacitated spermatozoa. While it is possible that such changes may reflect loading and/or staining differences between the two samples, an alternative explanation is that there is a relative increase in the abundance of these complexes following capacitation. The latter interpretation was further investigated through the use of quantitative densitometric analysis of the relative staining intensity of each of the major complexes between non-capacitated and capacitated samples (Fig. S2). Despite minor variations in protein loading, these data support the notion that a subset of protein complexes are differentially expressed (beyond that of the loading differences) following capacitation. Interestingly, the capacitation of human spermatozoa was also associated with a dramatic increase in the expression of phosphotyrosine in several of the high molecular weight complexes (Fig. 3B).

Given our interest in identifying proteins involved in zona adhesion, we next examined whether any of the protein complexes were expressed on the surface of the cell. For the purpose of these studies, populations of live capacitated human spermatozoa were labeled with a membrane-impermeable derivative of biotin. Native lysates were then resolved by BN-PAGE, transferred to nitrocellulose membranes and affinity labeled with HRP-conjugated streptavidin.

As shown in Fig. 3C, a subset of at least seven complexes were strongly labeled with biotin (arrowheads) suggesting that at least a portion of their constituent proteins are exposed on the surface of the cell. The specificity of the surface biotinylation reaction was indicated by the fact that there was no direct correlation between the relative abundance of each complex and the degree to which they were labeled with biotin. Further, we failed to detect recognized intracellular markers among any of the biotinylated complexes. In this respect, antibodies against cytosolic (tubulin), and mitochondrial (respiratory chain Complex IV) proteins consistently failed to cross-react with any of the putative complexes, while a protein predominately expressed on the sperm surface (CD59) showed cross-reactivity with at least two bands, both of which appear to correspond to those labeled in the biotinylation assay (Fig. S3). The notable detection of an additional biotinylated band (Fig. 3C, denoted by *) that did not appear to co-migrate with those stained in BN-PAGE gels (Fig. 3A), presumably reflects the greater sensitivity afforded by this technique over that of Coomassie blue staining.

Human sperm multimeric protein complexes bind homologous zona pellucidae

Having generated some of the first direct evidence for the expression of multimeric protein complexes on the surface of human spermatozoa, studies were next undertaken to explore the functional significance of these entities, particularly in relation to sperm–zona pellucida interaction. To facilitate these studies, native sperm lysates resolved by BN-PAGE were subjected to Far Western blotting with solubilized human zonae pellucidae. Following high stringency washing, at least five predominant protein complexes were identified that possessed affinity for the homologous zona pellucida proteins (Fig. 3D). As expected, the majority of these complexes co-migrated with a subset of those that were accessible to surface biotinylation. It is notable however, that one of these

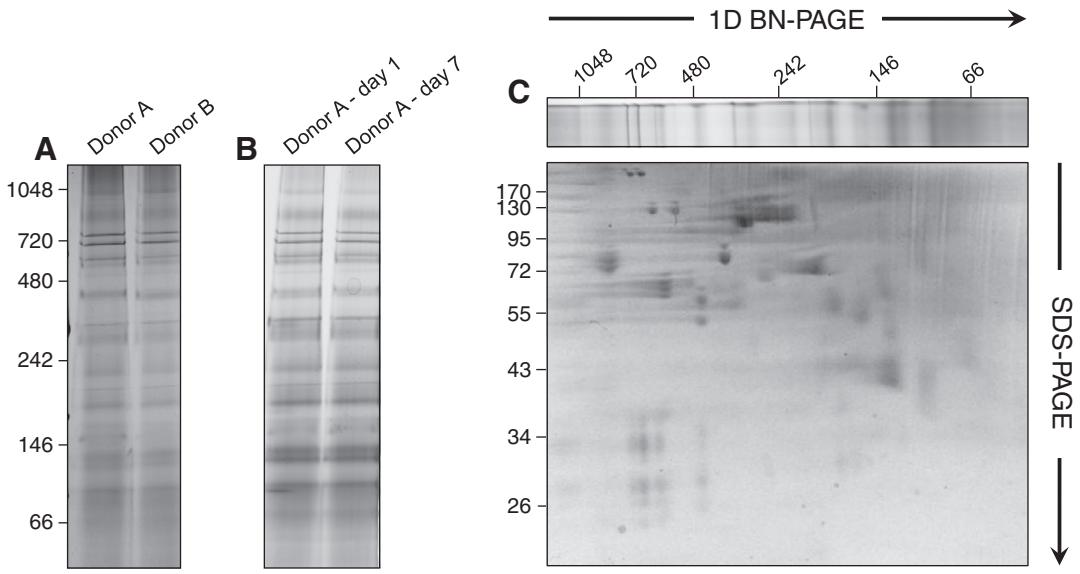

Fig. 2. Resolution of multimeric protein complexes from human spermatozoa. Purified populations of human spermatozoa were collected from (A) different donors or (B) different ejaculates of the same donor and incubated in capacitating media for 3 h. The cells were then solubilized in blue native lysis buffer and the extracted proteins were resolved on precast 4–16% BN-PAGE gels. The similarity in protein profiles between all samples attests to the reproducibility of the BN-PAGE protocol and the absence of significant inter- or intra-donor variability. (C) To confirm that the high molecular weight entities resolved by BN-PAGE were composite assemblages of multiple proteins, a single lane of a BN-PAGE gel was excised and embedded atop a standard 10% SDS-PAGE gel. Individual proteins were then resolved and stained with Coomassie G-250. Vertically aligned spots indicate the composition of each of the protein complexes, with the larger complexes being located on the left hand side of the image. Each experiment was replicated a minimum of three times and representative gels are shown. The numbers on the left of panels A and C correspond to the molecular weight (kDa) of Native-PAGE and SDS-PAGE protein standards, respectively.

complexes (approximately 300 kDa) failed to label with biotin in live spermatozoa (Fig. 3A, denoted by #). While it is difficult to refute the possibly that the labeling of this intracellular complex is non-specific, it is also feasible that it may contain proteins that are only exposed following the completion of acrosomal exocytosis and thereafter participate in secondary zona binding (Morales et al., 1989).

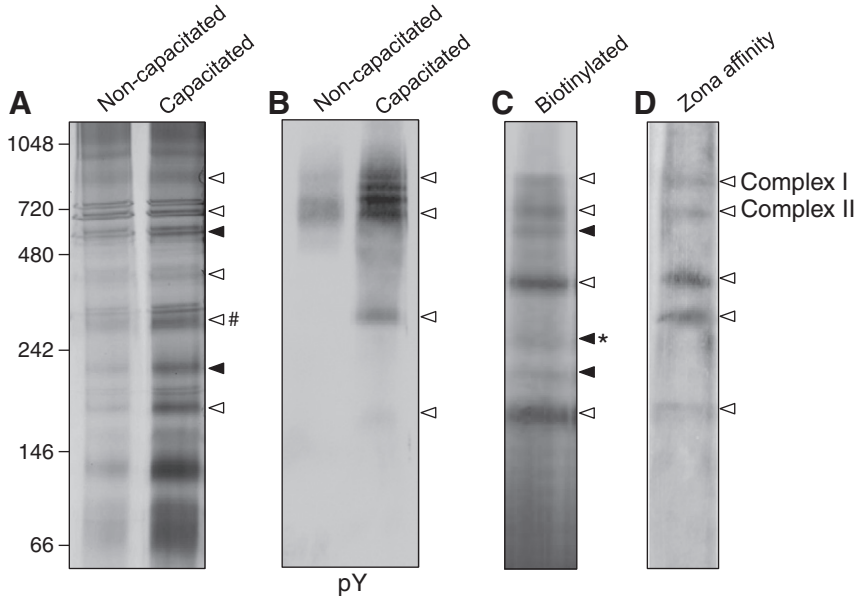

Fig. 3. Characterization of human sperm protein complexes. (A) To investigate the influence of the capacitation status on the expression of protein complexes in human spermatozoa, populations of non-capacitated and capacitated cells were solubilized in blue native lysis buffer and extracted proteins were resolved on precast 4–16% BN-PAGE gels. Although the qualitative profile of proteins remained similar between both populations, significant capacitation-associated changes were revealed in the relative levels of expression of several complexes. (B) Identical native lysates were also assessed for the expression of phosphotyrosine by immunoblotting with anti-phosphotyrosine antibodies. (C) To determine if any of these complexes were expressed on the surface of capacitated human spermatozoa, the cells were labeled with a membrane impermeable derivative of biotin prior to extraction and resolution of the native protein complexes. Biotinylated proteins were then detected by affinity labeling with HRP-conjugated streptavidin. (D) The ability of human sperm protein complexes to bind homologous zona pellucida was assessed by Far Western blotting. For this purpose, Western blots of native protein lysates were prepared from capacitated spermatozoa and then probed with solubilized, biotinylated zona pellucidae. Following washing, protein complexes with bound zonae were identified by affinity labeling with HRP-conjugated streptavidin. Each experiment was replicated a minimum of three times and representative gels and blots are shown. Arrowheads indicate the subset of biotinylated sperm surface protein complexes that either bound (unshaded) or failed to bind (shaded) homologous zona pellucidae. The single biotinylated protein complex that was not detected by BN-PAGE is denoted by an asterisk and the one protein complex that displayed ZP affinity but was not biotinylated is denoted by a # symbol. The high molecular weight complexes labeled Complexes I and II were selected for further characterization.

Table 1
Proteomic identification of individual components of Complexes I and II.

Protein (symbol)	UniProt accession number	Molecular weight (kDa)	Number of matched peptides	Mascot score
Complex I				
Chaperonin containing TCP-1 complex				
Subunit 1 (alpha) (CCT1)	P17987	60,306	2	108
Subunit 2 (beta) (CCT2)	P78371	57,488	2	40
Subunit 3 (gamma) (CCT3)	P49368	60,534	3	142
Subunit 4 (delta) (CCT4)	P50991	57,924	1	53
Subunit 5 (epsilon) (CCT5)	P48643	59,671	2	109
Subunit 6 (zeta 1) (CCT6A)	P40227	58,024	1	51
Subunit 7 (eta) (CCT7)	Q99832	59,329	7	182
Subunit 8 (theta) (CCT8)	P50990	59,621	1	66
Zona pellucida binding protein isoform 2 (ZPBP2)	Q6X784	38,652	1	58
Complex II				
Proteasome subunit				
Alpha type-1 (PSMA1)	P25786	29,556	21	427
Alpha type-2 (PSMA2)	P25787	25,899	16	405
Alpha type-3 (PSMA3)	P25788	28,433	20	297
Alpha type-4 (PSMA4)	P25789	29,484	18	473
Alpha type-5 (PSMA5)	P28066	26,411	11	392
Alpha type-6 (PSMA6)	P60900	27,399	18	510
Alpha type-7 (PSMA7)	O14818	27,887	24	366
Beta type-1 (PSMB1)	P20618	26,489	20	358
Beta type-2 (PSMB2)	P49721	22,836	19	293
Beta type-3 (PSMB3)	P49720	22,949	15	258
Beta type-4 (PSMB4)	P28070	29,204	16	576
Beta type-5 (PSMB5)	P28074	28,480	18	655
Beta type-6 (PSMB6)	P28072	25,358	10	195

Mass spectrometry analysis of zona pellucida adhesion Complexes I and II

In light of the promising data secured above we sought to substantiate the zona binding affinity of the isolated complexes by focusing on the identification of their individual subunits. Specifically, Complexes I and II (Fig. 3D), which not only showed affinity for the ZP but were also surface expressed, were selected for tandem mass spectrometry analysis using a 1D nano LC-ESI MS/MS interface.

The sequencing of Complex I revealed the presence of the eight subunits that comprise the cytosolic chaperonin containing TCP-1 (CCT) complex, in addition to the putative zona recognition molecule, zona pellucida binding protein isoform 2 (ZPBP2) (Table 1). Interestingly, a complex comprising the same cohort of proteins has recently been identified in mouse spermatozoa and implicated in zona adhesion in this species (M. Dun, unpublished observations). Given that the combined molecular weight of the TCP-1 complex and ZPBP2 is less than 600 kDa, it is likely that this approximately 900 kDa complex accommodates additional proteins that were not identified in our initial mass spectrometry analysis. Unfortunately however, additional attempts to sequence the remaining proteins were not successful.

A similar sequencing strategy for Complex II led to the identification of the seven α-subunits and six of the seven β-subunits that comprise the 20S proteasome (Table 1). With individual molecular weights of approximately 20–30 kDa, the collective mass of the identified proteasome subunits totals 350 kDa, half that of the observed size of Complex II (700 kDa). Such results again suggest that the entire complement of proteins within Complex II were not sequenced. However, given that the predicted molecular weight of the full 20S proteasome is 700 kDa it is considered very likely that Complex II represents the complete 20S proteasome, a conclusion supported by immunoblotting experiments (see below).

Validation of the proteomic composition of Complexes I and II

In order to confirm the presence of the TCP-1 complex and ZPBP2 in Complex I, commercial antibodies generated against four of the individual CCT subunits (CCT2, CCT3, CCT6A, and CCT8) and against ZPBP2 were sourced for use in probing immunoblots of 1D BN-PAGE

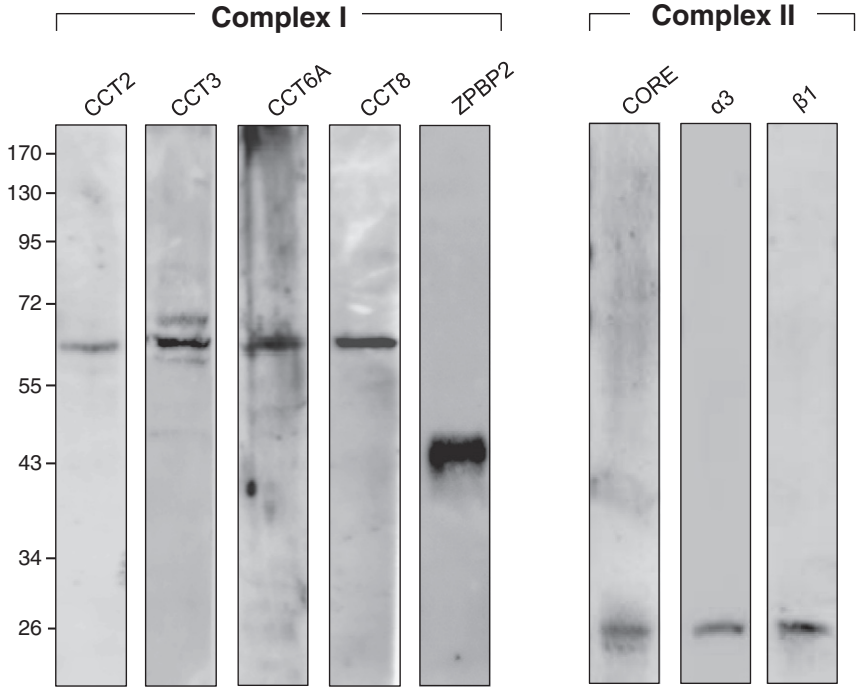

Fig. 4. Validation of the specificity of the antibodies against proteins of interest. The specificity of each of the commercial antibodies used in this study was confirmed by immunoblotting against protein extracts prepared by solubilization of human spermatozoa in SDS extraction buffer. The four antibodies sourced against the subunits of the TCP-1 complex (CCT2, CCT3, CCT6A and CCT8) labeled a predominant protein of ~60 kDa. Anti-ZPBP2 antibodies also labeled a single, diffuse band of ~45 kDa. A suite of 14 antibodies generated against the alpha and beta subunits of the 20S proteasome recognized proteins of the predicted molecular weight (between 20 and 30 kDa). Representative immunoblots for three of these antibodies (core: recognizes several members of the 20S proteasome catalytic core; alpha 3 subunit: component of the outer rings; and beta 6 subunit: component of the inner rings) are shown for this complex.

gels. Prior to these studies, however, the specificity of each of the antibodies was validated by immunoblotting of SDS extracts human spermatozoa using standard SDS-PAGE (Fig. 4).

The antibodies against the four CCT subunits displayed appropriate affinity for a predominant protein band of 60 kDa. Similarly, the anti-ZPBP2 antibody labeled a single, diffuse band of ~45 kDa, slightly higher than that of the predicted molecular weight of ZPBP2 (38 kDa), a fact that may be attributed to the glycosylation of the core protein. As anticipated, these antibodies also displayed strong labeling of a high molecular weight protein band (900 kDa) corresponding to that of Complex I in native extracts prepared from capacitated spermatozoa and analyzed by BN-PAGE (Fig. 5A,B). Although modest cross-reactivity with other bands was observed with several of the CCT antibodies, Complex I was the only band consistently recognized by the entire panel of antibodies. Furthermore, immunoblotting of 2D BN-PAGE gels confirmed the specificity of this labeling with proteins of the anticipated molecular weight (~60 kDa) being observed in alignment with Complex I, when the complexes were resolved in the second dimension under denaturing conditions (Fig. 5D). In addition to Complex I, anti-ZPBP2 antibodies also displayed relatively strong labeling of a second complex of approximately 500 kDa and weaker labeling of additional lower molecular weight complexes (Fig. 5B). Such findings raise the possibility that ZPBP2 may interact with additional proteins other than those of the TCP-1 complex. This conclusion was supported by immunoblotting of 2D BN-PAGE gels which confirmed that a protein of the appropriate molecular weight for ZPBP2 aligned with at least 5 complexes, notwithstanding its clear localization in Complex I (Fig. 5E).

A similar approach was also employed to validate the presence of 20S proteasome complex in human spermatozoa. The specificity of a suite of commercial antibodies against all 14 subunits of the 20S proteasome was again demonstrated by immunoblotting against whole human sperm lysates (Fig. 4). In each case the antibodies demonstrated affinity for proteins of the predicted molecular weight (between 20 and 30 kDa), confirming the recent proteomic profiling of human spermatozoa, which also detected the complete proteasome complex (Baker et al., 2007). Similarly, the anti-proteasome antibodies also confirmed the presence of each subunit within Complex II (Fig. 5C). However, instead of the anticipated single band at 700 kDa, each of the 14 antibodies, illustrated by the anti-'core', anti-α3 and anti-β1 antibodies, consistently labeled a triplet of high molecular weight complexes of approximately 680, 700 and 750 kDa (Fig. 5C). Similarly, immunoblotting of 2D BN-PAGE gels confirmed that proteins of the appropriate molecular weight for the proteasome subunits aligned with each of these three complexes (Fig. 5F).

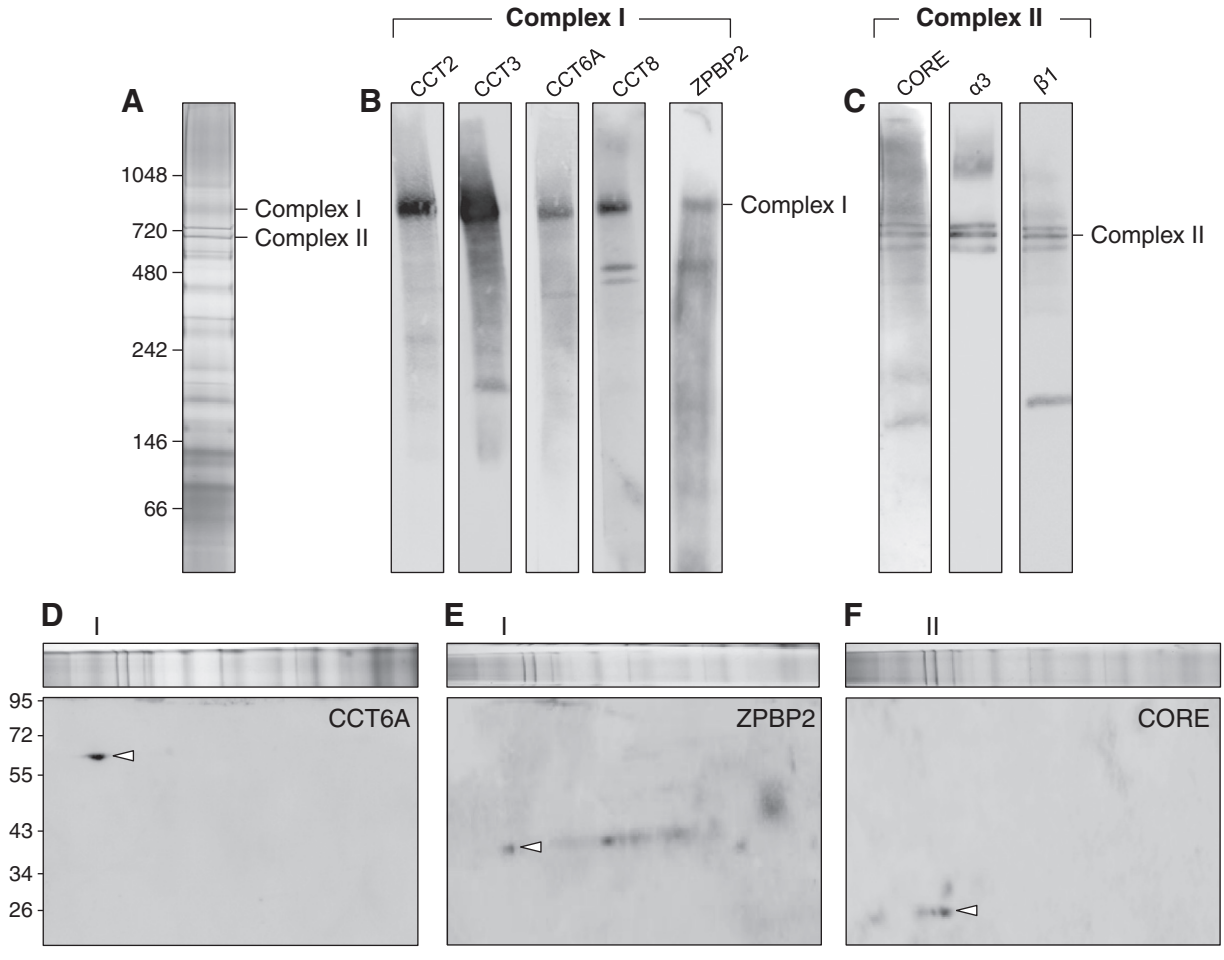

Fig. 5. Validation of the proteomic composition of Complexes I and II. (A) Native protein complexes were extracted from capacitated human spermatozoa and resolved by BN-PAGE. These samples were then prepared for immunoblotting with a panel of antibodies selected on the basis of LC–MS/MS sequence analysis of (B) Complex I (CCT2, CCT3, CCT6A, CCT8, and ZPBP2) and (C) Complex II (20S proteasome: core, α3 subunit, and β1 subunit). (D–F) The specificity of labeling in 1D-PAGE immunoblots was confirmed by 2D BN-PAGE, whereby a single lane of a 1D BN-PAGE was placed atop an SDS-PAGE gel and the individual proteins within each complex were resolved according to their molecular weight. These gels were then prepared for immunoblotting with (D) anti-CCT6A, (E) anti-ZPBP2 or (F) anti-20S proteasome core antibodies. Each of these experiments was repeated three times and representative gels and Western blots are shown. The arrowhead in panels D–F indicates the position of labeled proteins vertically aligned with Complexes I and II.

Localization of the proteins comprising Complexes I and II

Following confirmation of the proteomic composition of Complexes I and II, the cellular localization of these proteins was examined in populations of non-capacitated and capacitated human spermatozoa. Although these studies were initially attempted in live spermatozoa, the staining of these cells proved problematic presumably due to membrane damage induced by the multiple washing steps required by the labeling protocol. Hence the images shown in Figs. 6–8 are of spermatozoa that were fixed in 4% paraformaldehyde prior to antibody labeling. As a consequence, these analyses were capable of generating important information on the cellular domain harboring the target antigens but could not determine whether the expression was intracellular or on the sperm surface. In performing these analyses we also sought to simultaneously assess the acrosomal status of these cells using TRITC conjugated PNA. In non-capacitated spermatozoa, three of the four CCT subunits (CCT2, CCT6A and CCT8) examined co-localized in the peri-acrosomal region of the sperm head in addition to faint labeling in the flagellum (Fig. 6). A similar pattern of CCT6A and CCT8 localization was observed in the head of capacitated spermatozoa, however principal piece staining for both proteins was markedly reduced in these cells, although CCT6A was still expressed in the sperm midpiece. Capacitation also induced a striking relocalization of CCT2 such that the protein could no longer be detected in the peri-acrosomal region but was instead found within the equatorial segment of the sperm head. The persistence of PNA labeling in these cells suggests that these altered patterns of localization were not induced by acrosomal exocytosis. Interestingly, in the case of CCT3 only very weak labeling was detected in non-capacitated spermatozoa. The staining intensity for this subunit increased following capacitation whereupon CCT3 appeared to be distributed in the peri-acrosomal region and flagellum. Importantly, the representative patterns described were observed in more than 80% of each sperm sample examined, with no notable inter- or intra-donor variability.

As demonstrated in Fig. 7A, ZPBP2 was also localized to similar regions within the sperm head as a majority of the CCT subunits, with strong peri-acrosomal labeling noted in both non-capacitated and capacitated spermatozoa. Modest staining of the midpiece was also detected; however, the principal piece of the flagellum consistently failed to label with anti-ZPBP2 antibodies. Co-localization of ZPBP2 with the subunits of the TCP-1 complex was confirmed by dual labeling of capacitated human spermatozoa with anti-CCT and anti-ZPBP2 antibodies. As anticipated, with the exception of CCT2, overlapping patterns of CCT and ZPBP2 expression were detected within the peri-acrosomal region of the capacitated sperm head (Fig. 7B).

In addition to examining the expression of the components of Complex I, antibodies against the 20S proteasome subunits were used to similarly validate the expression of this complex (Complex II) within a region of human spermatozoa compatible with a putative role in zona pellucida interactions. With a few minor exceptions, fixed human spermatozoa incubated with each of the anti-proteasome subunit antibodies exhibited similar patterns of labeling. In this regard,

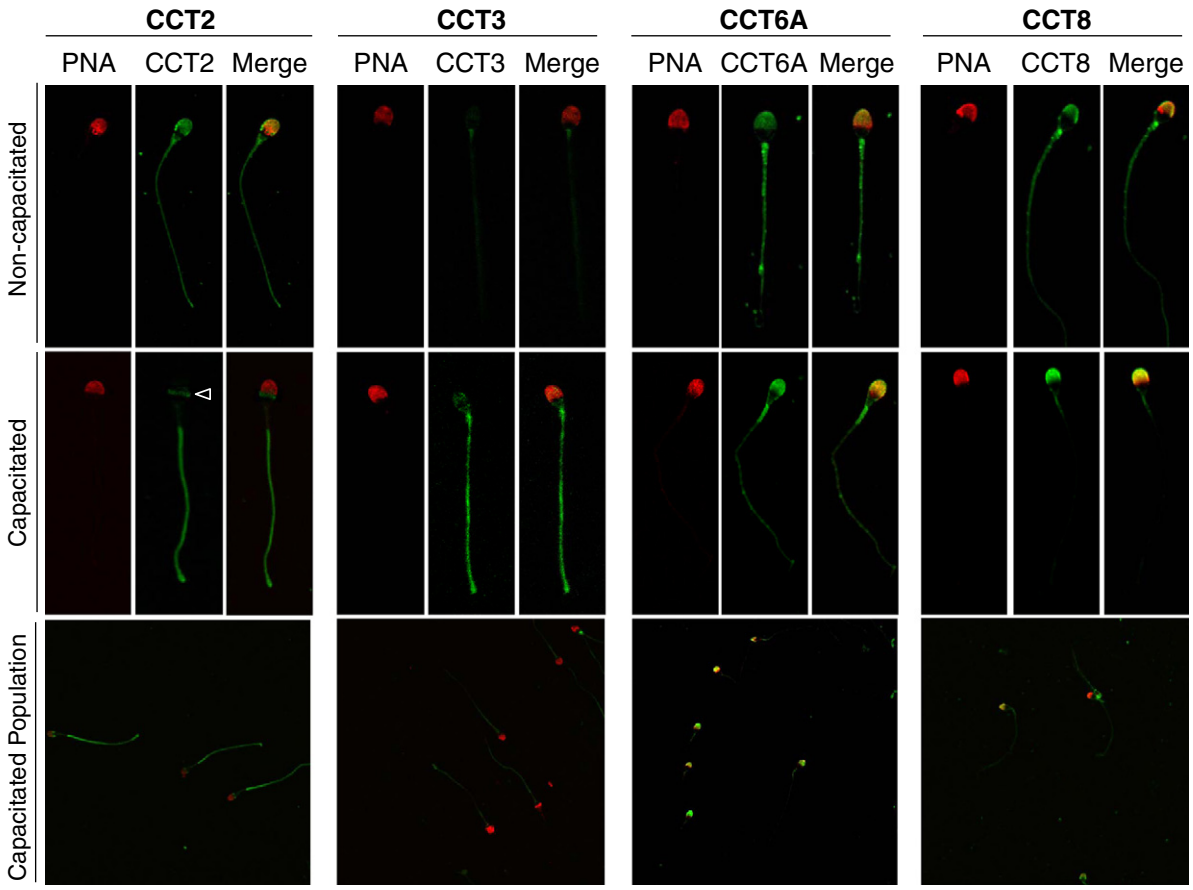

Fig. 6. Localization of the TCP-1 complex subunits in human spermatozoa. Capacitated and non-capacitated populations of human spermatozoa were fixed with 4% paraformaldehyde prior to sequential labeling with antibodies against CCT2, CCT3, CCT6A or CCT8 and a FITC-conjugated secondary antibody (green). The cells were subsequently counter-stained with TRITC-conjugated PNA (red) to assess acrosome integrity. Negative controls were performed by incubating cells with secondary antibody only and, as anticipated these revealed no staining beyond relatively weak background fluorescence (data not shown). This experiment was replicated three times using pooled semen samples and representative images are shown.

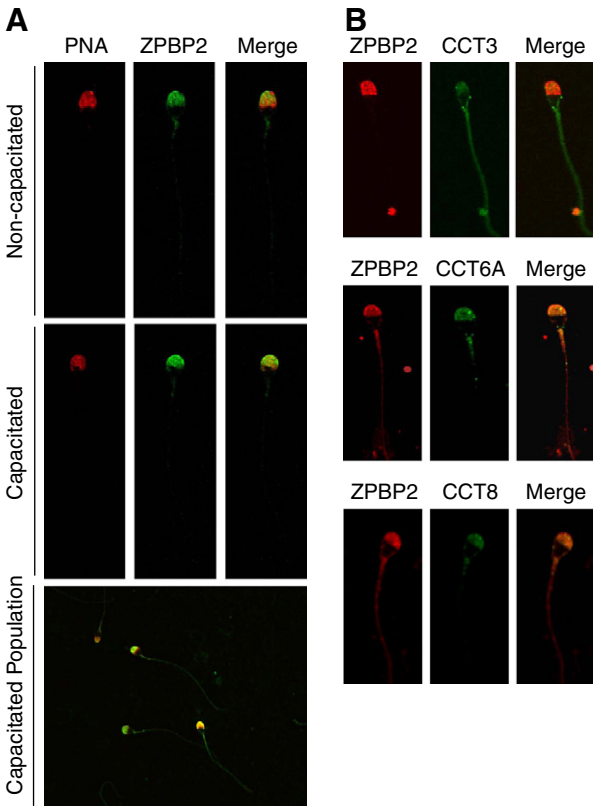

Fig. 7. Localization of ZPBP2 in human spermatozoa. (A) Capacitated and non-capacitated populations of human spermatozoa were fixed with 4% paraformaldehyde prior to sequential labeling with antibodies against ZPBP2 and a FITC-conjugated secondary antibody (green). The cells were subsequently counter-stained with TRITC-conjugated PNA (red) to assess acrosome integrity. (B) To confirm the interaction of ZPBP2 with the TCP-1 complex, populations of human spermatozoa were dual labeled with anti-ZPBP2 (red) followed by anti-CCT3, -CCT6A or -CCT8 antibodies (green). These experiments were replicated three times using pooled semen samples and representative images are shown.

proteasome immunoreactivity localized strongly to the neck and anterior midpiece (Fig. 8). Labeling was also generally detected, albeit of lower intensity, along the flagellum and throughout the peri-acrosomal region of the head. Interestingly the α3 subunits were strongly expressed within the flagellum but could not be detected within the sperm head (Fig. 8). Importantly, the expression patterns of the various subunits examined did not display any marked inter- or intra-donor variability, nor did they change dramatically in populations of either non-capacitated or capacitated spermatozoa. The specificity of the various labeling patterns was demonstrated by the absence of labeling in control samples prepared in the absence of either the primary and/or secondary antibodies (results not shown).

Validation of the association between the TCP-1 complex and ZPBP2

Given the novelty and potential significance of surface expressed complexes containing the zona adhesion molecule, ZPBP2, and TCP-1 chaperonins, two complementary strategies were adopted to confirm this interaction. Firstly, a representative anti-CCT antibody (anti-CCT6A) was used to co-immunoprecipitate interacting proteins from sperm lysates and secondly, this antibody was used in conjunction with an *in situ* proximity ligation assay (Duolink) to further validate the *in vivo* interaction of these proteins in human spermatozoa. To conduct the pull down studies we first confirmed that the anti-CCT6A antibodies successfully immunoprecipitated this component of the chaperonin complex (Fig. 9A). When these blots were stripped and reprobed with anti-ZPBP2 antibodies, a cross reactive band was clearly detected, confirming the close association of this molecule with the chaperonin complex (Fig. 9B). Similarly, the proximity ligation assay confirmed a specific co-localization of ZPBP2 and CCT6A (Fig. 9C). As anticipated, the fluorescent signal produced as a consequence of this interaction appeared as a number of discrete spots that were restricted to the peri-acrosomal region of the sperm head in >85% cells examined. No co-localization was observed in any other region of the spermatozoa. In addition to CCT6A, we also investigated the putative interaction between ZPBP2 and other TCP-1 subunits (*i.e.* CCT3 and CCT8) and confirmed that all three produced similar results in proximity ligation assays (results not shown). These findings are consistent with those observed in the co-localization experiments described above (Fig. 7B). The specificity of this labeling pattern was confirmed through the use of anti-CCT6A and an irrelevant antibody (anti-α-tubulin) that was an isotype match for anti-ZPBP2. Similarly, this experiment was also conducted in the absence of either anti-CCT6A and/or anti-ZPBP2. As anticipated, none of the control treatments produced any fluorescent signals.

Complexes I and II possess affinity for homologous zonae pellucidae

In order to secure evidence in support of the role of Complexes I and II in zona adhesion, capacitated spermatozoa were pre-incubated with antibodies directed against key components of the respective complexes prior to assessing their ability to engage in zona binding. Alternatively, native sperm lysates were isolated and incubated with zona-intact oocytes. Following incubation, the oocytes were subjected to stringent washing and then immunolabeled with appropriate antibodies to determine if either complex of interest was capable of adhering to native zonae.

In the case of Complex I, pre-incubation of human spermatozoa with anti-ZPB2 antibodies significantly ($P<0.05$) reduced their ability to bind to zona intact human oocytes (Fig. 10A). In contrast, anti-CCT2 antibodies elicited only a modest reduction in sperm–ZP interaction (Fig. 10A). Immunolabeling of oocytes following incubation with preparations of native sperm lysates confirmed that representative subunits of Complex I (CCT2 and ZPBP2) did in fact adhere to the zonae (Fig. 10B). Although we also observed labeling of the oocyte in this experiment, this staining persisted in control samples incubated without primary antibody (Fig. 10B). From these data we infer that the oocyte labeling is most likely an artifact attributed to non-specific secondary antibody labeling, a phenomenon we have also observed in previous studies (Nixon et al., in press). In contrast, the zona pellucida was only weakly labeled in these control samples (Fig. 10B). The specificity of zona binding was further demonstrated by the fact that pre-incubation of the native lysates with anti-ZPBP2 antibodies dramatically reduced the amount of CCT2 labeling subsequently detected on the zonae (Fig. 10B). Such results confirm that ZPBP2 is a key determinant of the zona affinity associated with Complex I. In contrast, pre-incubation of the native lysate with anti-CCT2 antibodies failed to reduce the amount of ZPBP2 labeling (Fig. 10B).

The application of a similar experimental strategy confirmed that the 20S proteasome complex (Complex II) also possessed zona affinity. In this context it was demonstrated that pre-incubation of human spermatozoa with antibodies against representative 20S proteasome subunits (anti-α3 and anti-β1) significantly inhibited their ability to bind to zona intact human oocytes (Fig. 10A). Similarly, strong labeling of the proteasome complex (anti-core) was detected on zonae pellucidae following incubation of oocytes with native sperm lysates. However, this binding was virtually eliminated if the oocytes were incubated with anti-ubiquitin antibodies, to mask the ligands for proteasome adhesion, prior to the addition of the native sperm lysates (Fig. 10B).

Discussion

The extraordinary complexity of the molecular interactions that underpin the adhesion of a spermatozoon to the outer vestments of an

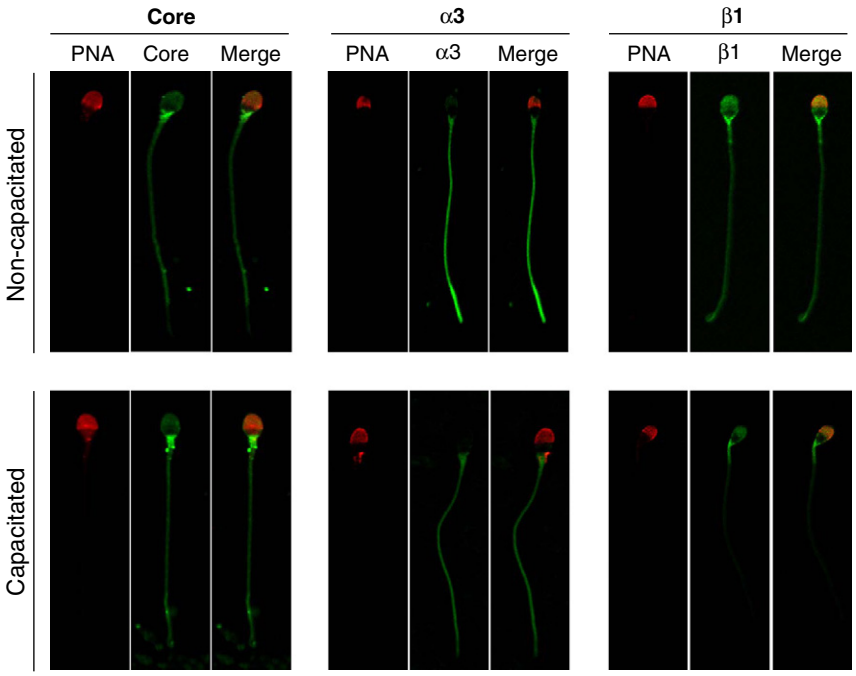

Fig. 8. Localization of the 20S proteasome subunits in human spermatozoa. Capacitated and non-capacitated populations of human spermatozoa were fixed with 4% paraformaldehyde prior to sequential labeling with anti-core proteasome, anti-α3 or anti-β1 antibodies, respectively (green). The cells were then counter-stained with TRITC-conjugated PNA (red) to assess acrosome integrity. Negative controls were performed by incubating cells with secondary antibody only and revealed minimal background fluorescence (data not shown). This experiment was replicated three times using pooled semen samples and representative images are shown.

ovulated oocyte is becoming increasingly apparent. In a situation that draws interesting parallels with many somatic cell–cell interactions, we provide the first direct evidence that human spermatozoa employ a suite of multi-molecular protein complexes to mediate their interactions with homologous zonae pellucidae. Such a finding is perhaps not surprising given that many vital cellular functions are underpinned by structured complexes of proteins working in concert, rather than freely diffusing or randomly colliding proteins (Alberts, 1998). In fact, recent advances in functional proteomics have revealed that most proteins fulfill their functional potential in multi-protein complexes (MPCs) and that the human proteome alone contains approximately 10^4 different MPCs (Sali et al., 2003). Further, there are an impressive number of examples of cells that employ MPCs to engage in cellular adhesions events. For example, cell–cell contact in barrier-forming epithelial and endothelial cells is tightly regulated by an array of MPCs that are assembled along lateral cell junctions. In such cells, each MPC often fulfills a unique functional role, and recent evidence suggests that their composition is dynamic and regulated by a number of factors including contact-induced aggregation, conformational changes, phosphorylation, and tension (Ebnet, 2008; Shen et al., 2008). By analogy, the presence of many sperm complexes that exhibit zona binding affinity (Fig. 3D) raises the possibility that such supramolecular assemblages may participate in sequential or hierarchical molecular interactions with the zona pellucida. Alternatively, these complexes may act in a synergistic manner to ensure the success of this pivotal cellular interaction. Support for the former conclusion rests with our characterization of two biochemically distinct complexes which may both contribute to sperm–zona interaction *via* different mechanisms.

The first of these, Complex I, was shown to comprise members of the TCP-1 complex (CCT1–CCT8) (Table 1), a cohort of proteins that, to the best of our knowledge, have not previously been identified in human spermatozoa. The fact that this is a recognized complex of proteins argues against the possibility that BN-PAGE induces artifactual protein associations and instead suggests that we were successful in our attempt to isolate physiologically relevant assemblages of proteins. In somatic cells, the TCP-1 complex is constructed as a double-ring structure consisting of eight unique subunits that surround a central cavity. This cavity provides a favorable environment for protein folding and enables the TCP-1 complex to fulfill its primary role as a molecular chaperone. The complex is in fact relatively promiscuous, with conservative estimates suggesting that it assists in the correct folding of approximately 5–10% of the cellular proteome (Camasses et al., 2003; Feldman et al., 1999; Gomez-Puertas et al., 2004; Guenther et al., 2002; Kubota et al., 2006; Leroux and Hartl, 2000; Sternlicht et al., 1993; Won et al., 1998). Interestingly, the original TCP-1 subunit (CCT1) was first identified as a highly expressed mouse testicular protein (Silver, 1985) encoded by a gene located within a variant region of chromosome 17, known as the t-complex (Silver et al., 1979). This region is of particular interest as it is known to harbor a number of genes that are important for mouse development and fertility, including: sperm motility (Olds-Clarke and Johnson, 1993; Pilder et al., 2007), the ability to capacitate (Si and Olds-Clarke, 1999) and importantly, the ability to bind to and penetrate the zona-pellucida (Johnson et al., 1995; Si and Olds-Clarke, 1999). Indeed, male mice that carry two t haplotypes are invariably sterile due to lesions in at least one of these sperm attributes.

Within the testes, the TCP-1 complex has been implicated in the extensive reorganization of the microtubular cytoskeleton that occurs during cytodifferentiation of haploid spermatids into spermatozoa (Soues et al., 2003). However, its functional role in morphologically mature spermatozoa has not previously been examined. Consistent with the findings of the present study, work in the mouse has shown that the TCP-1 complex is expressed within the apical region of the sperm head and from this position is able to participate indirectly in sperm–ZP interactions (M. Dun, personal communication). The modest reduction in sperm–ZP binding observed after incubation of human spermatozoa with anti-CCT2 antibodies in the present study lend further support to this interpretation. One possibility that could account for such findings is that the TCP-1 complex is responsible for the presentation, stabilization and/or assembly of zona adhesion molecule (s). This notion is in keeping with findings that the TCP-1 complex can regulate the formation of multiprotein complexes (Feldman et al., 1999; Guenther et al., 2002). Among the putative TCP-1 client proteins that could account for the zona affinity of Complex I, we have identified zona

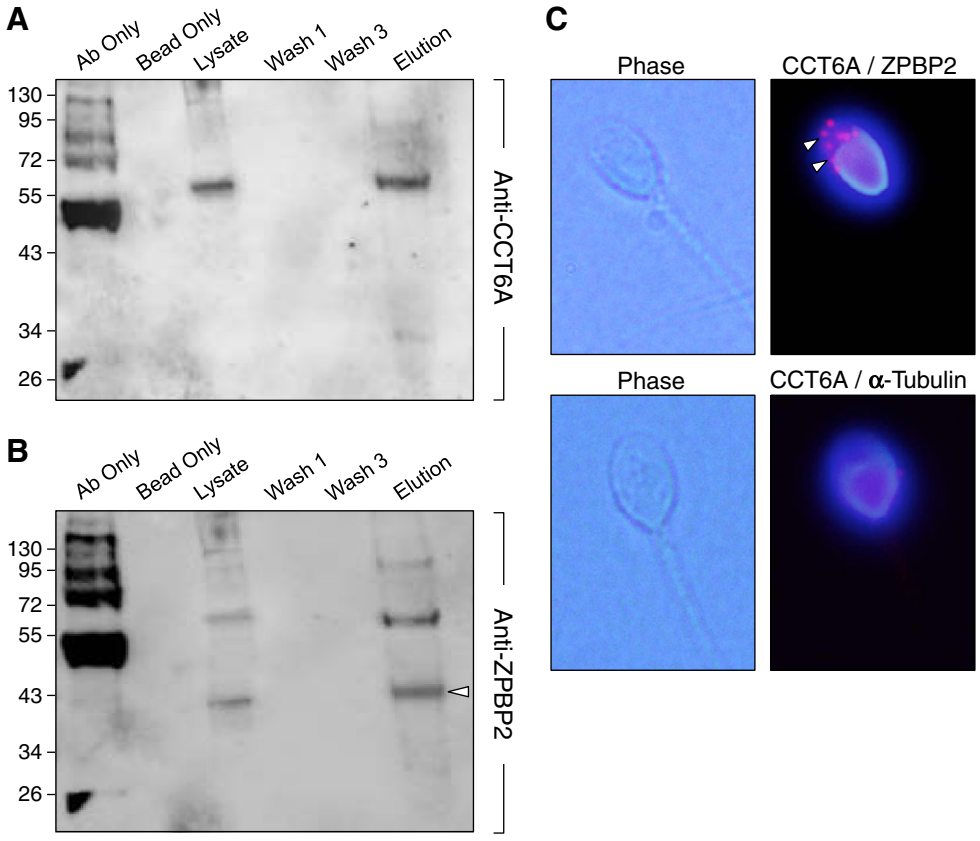

Fig. 9. Examination of TCP-1/ZPBP2 interaction. Capacitated human spermatozoa were solubilized in immunoprecipitation lysis buffer and the lysates incubated overnight at 4 °C with Protein G Dynabeads conjugated with anti-CCT6A antibodies. The beads were then boiled in SDS, and the immunoprecipitates were resolved on 10% SDS-PAGE gels and transferred to nitrocellulose membranes. Membranes were probed with (A) anti-CCT6A antibodies to confirm the efficacy of immunoprecipitation before being stripped and (B) reprobed with anti-ZPBP2 antibodies. Although the stripping protocol failed to remove all of the bound CCT6A antibody, an additional band corresponding to ZPBP2 was detected in the elution lane in the latter blots (arrowhead). Control samples included an antibody only control in which antibody conjugated beads were incubated in the absence of cell lysates and a bead only control in which beads were incubated with capacitated sperm lysates in the absence of antibody. A whole sperm lysate was included to confirm the identity of the co-precipitated proteins as was the material recovered after washing the beads to confirm the specificity of the elution. This experiment was replicated three times using pooled semen samples and representative blots are depicted. (C) Capacitated human spermatozoa were fixed in 2% paraformaldehyde and allowed to settle onto poly-L-lysine slides. These samples were then blocked, followed by incubation with primary antibodies (anti-CCT6A and ZPBP2; anti-CCT6A and anti-tubulin) overnight at 4 °C, and oligonucleotide-conjugated secondary antibodies (PLA probes) for 1 h at 37 °C. The PLA probes were then ligated and the signal was amplified according to the manufacturer's instructions before being viewed using fluorescence microscopy.

pellucida binding protein 2 (ZPBP2) as a compelling candidate. The novel interaction between the TCP-1 complex and ZPBP2 was confirmed by co-immunoprecipitation, co-localization and proximity ligation assays. In the latter assay, the detection of a small number of discrete complexes (approximately 10/sperm) may indicate that while both proteins are present in the peri-acrosomal region of the sperm head, only a portion of these oligomerize to form complexes.

ZPBP2 is a paralogue of zona pellucida binding protein 1 (ZPBP1) (Mori et al., 1993), a protein originally implicated in secondary ZP binding. However, recent evidence from knockout models suggests the two proteins have distinct functions in spermatozoa. In this respect, male mice null for ZPBP1 are infertile due to defects in spermatogenesis that manifest in the form of poor acrosome compaction, abnormal head morphology and an inability to swim in a forward progressive manner. In contrast, male mice null for ZPBP2 display subfertility associated with defects in ZP interaction and penetration (Lin et al., 2007). To date, neither ZPBP1 nor ZPBP2 has been characterized in human spermatozoa. However, the conservation of the latter protein and its interaction with the TCP-1 complex in both human and mouse spermatozoa suggests that it may be of general significance in the mediation of sperm–ZP interaction. In this context, it is well established that sperm–ZP engagement can be resolved into both low and high affinity interactions and that the former of these is likely to employ sperm surface molecules that are conserved across species (Nixon et al., 2007). The importance of ZPBP2 as a key determinant of the zona affinity associated with Complex I was demonstrated by the ability of anti-ZPBP2 antibodies to potently inhibit the zona binding affinity of this native complex. In contrast, the reciprocal experiment in which native sperm lysates were incubated with anti-CCT2 antibodies did not elicit a comparable inhibition of ZPBP2 interaction with the zonae. From these data we infer that the CCT subunits of Complex I are indirectly involved in zonae adhesion (see above) or alternatively, that ZPBP2 is capable of functioning as a monomer or in concert with additional zona adhesion complexes. Support for the latter conclusion rests with the demonstration that ZPBP2 does resolve into a number of high molecular weight complexes by BN-PAGE (see Fig. 5B,E).

The capacitation status of spermatozoa did not appear to overtly influence either the relative abundance or the molecular weight of Complex I, thus indicating the complex is likely to be assembled prior to the induction of capacitation. These data pose an interesting dichotomy given that non-capacitated spermatozoa do not possess the ability to bind zonae pellucidae. One explanation for these conflicting observations is that the subunits of Complex I may be the subject of capacitation-dependent post-translational modifications that confer additional biological activity. In support of this model, our results indicate that there is an apparent increase in the levels of phosphotyrosine expression associated with Complex I during capacitation (Fig. 3B). This finding takes on added significance in view of the fact that phosphorylation of molecular chaperones has been causally linked to the exposure of novel binding

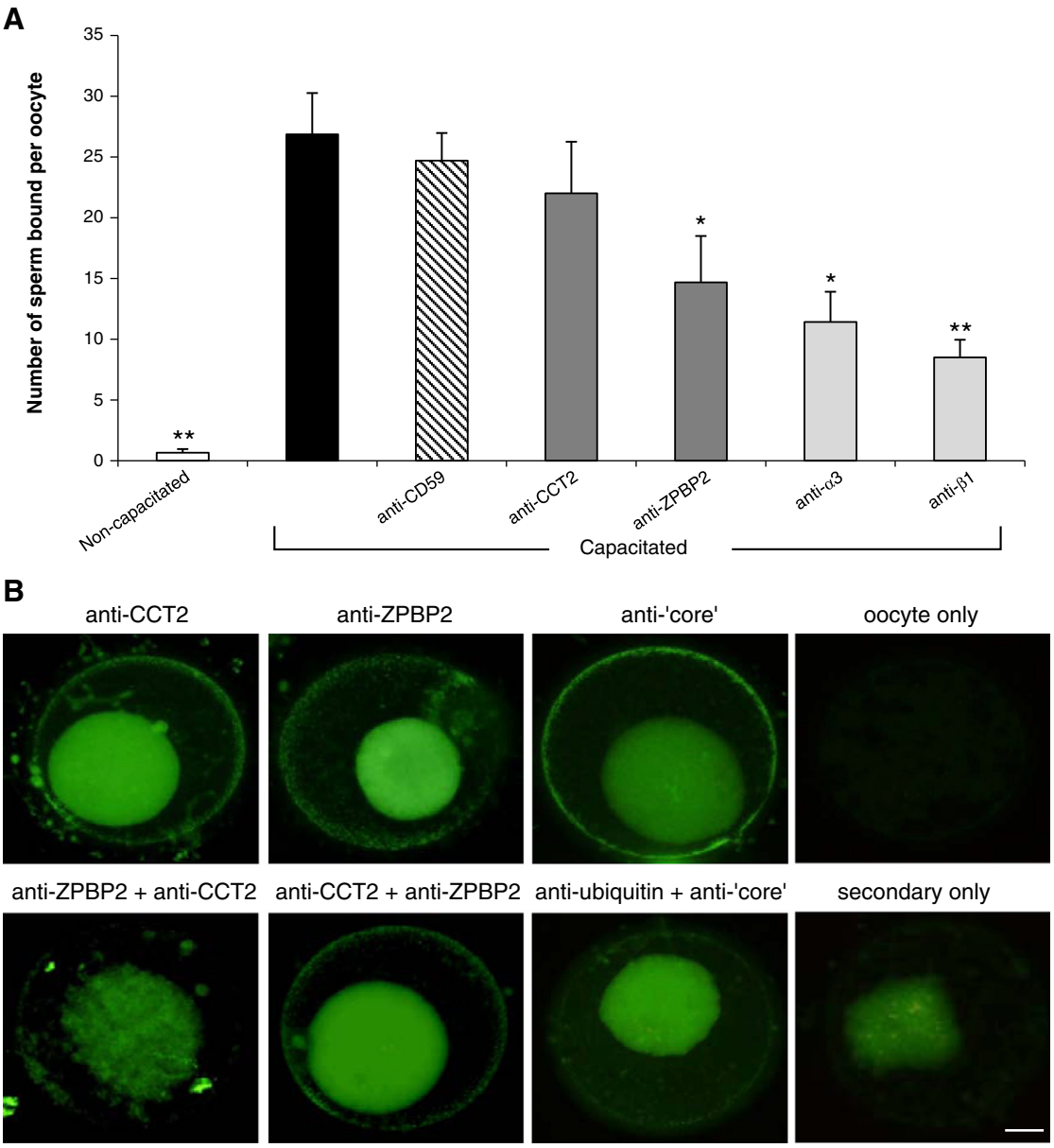

Fig. 10. Investigation of the role of Complex I and Complex II in sperm–zona pellucida interaction. (A) Capacitated spermatozoa were incubated with either anti-CCT2, anti-ZPBP2, anti-α3 or anti-β1 antibodies (diluted 1:100) for 30 min at 37 °C. The sperm suspensions were then washed and approximately 5×10^5 cells were placed in a droplet containing 4–8 salt stored oocytes. Oocytes were then washed to remove loosely bound spermatozoa, and the number of cells remaining bound to each zona was scored. An antibody directed against the sperm surface protein, CD59 (anti-CD59) was included as a control. (B) Native lysates were prepared from capacitated spermatozoa and incubated with oocytes for 30 min as described (Fig. S1). The oocytes were then sequentially labeled with anti-CCT2, anti-ZPBP2, or anti-proteasome core antibodies followed by FITC conjugated secondary antibodies. Alternatively, the native lysates were pre-treated with anti-ZPBP2 or anti-CCT2 prior to incubation with oocytes. These oocytes were then labeled with the reciprocal antibodies (anti-ZPBP2 + anti-CCT, anti-CCT2 + anti-ZPBP2). In the final treatment, oocytes were pre-incubated with anti-ubiquitin antibodies prior to the addition of the native lysate and probing with anti-proteasome core antibodies (anti-ubiquitin + anti-'core'). Negative controls for this experiment consisted of unlabeled oocytes (oocytes only), or oocytes labeled with secondary antibody only. In the latter samples, the oocytes, but not the zonae, were labeled suggesting that the former is an artifact attributed to non-specific secondary antibody labeling. Each experiment was replicated 3 times with a minimum of 5 oocytes per treatment and representative immunocytochemical images are shown (scale bar = 20 μm). Graphical data expressed as the mean ± s.e.m. *$P<0.05$, **$P<0.01$ compared with capacitated control.

surfaces, alterations in substrate preference, and their ability to interact with client proteins (Aquilina et al., 2004; Ecroyd et al., 2007; Thériault et al., 2004). It is also conceivable that the activity Complex I may be underpinned by dynamic remodeling or repositioning during capacitation (Asquith et al., 2004). However, this interpretation awaits further investigation.

Proteomic analysis of Complex II identified the majority of the subunits that comprise the 20S proteasome (Table 1), a large protease complex that is responsible for the selective degradation of ubiquitinated target proteins. Such findings again attest to the ability of BN-PAGE to isolate intact protein complexes from spermatozoa. One peculiarity of our study was the finding that the proteasome complex resolved as three large, but discrete bands in 1D BN-PAGE gels. Although the reason for this anomaly was not directly investigated, one possibility, supported by both our mass spectrometry data and anti-phosphotyrosine immunoblots (Fig. 3B), is that certain subunits of the complex may be subjected to post-translational modifications. Indeed, peptides corresponding to at least 9 subunits (α1–7, β1 and β4) displayed charge shift signatures characteristic of tyrosine phosphorylation. In this context, it is noteworthy that tyrosine phosphorylation of similar subunits has been shown to influence the substrate specificity of the complex in other cell types (Bose et al., 1999; Castano et al., 1996;

Mason et al., 1996; Wehren et al., 1996). Taken together, such findings raise the intriguing possibility that proteasome complexes may be differentially activated during sperm maturation in preparation for a functional role in sperm–oocyte interactions.

In agreement with previous work demonstrating that the proteasome complex is highly expressed within populations of epididymal spermatozoa we found no evidence that the capacitation status of spermatozoa altered the relative abundance of this complex. The presence of the ubiquitin–proteasome pathway has been well documented in the reproductive systems of a variety of invertebrate and mammalian species. For instance, the proteasome complex has been shown to be expressed in the spermatozoa of a number of species including human (Baker et al., 2007; Morales et al., 2003, 2004), mouse (Pasten et al., 2005) and pig. In addition, ubiquitinated substrates have also been detected in seminal plasma (Lippert et al., 1993), epididymal fluid (Hermo and Jacks, 2002; Sutovsky et al., 2001) on the surface of defective epididymal spermatozoa, as well as in follicular fluid (Einspanier et al., 1993), and on the outer surface of the zona pellucida (Sutovsky et al., 2004). Consistent with such findings, the ubiquitin–proteasome system has been implicated in various aspects of sperm–oocyte interactions (Sakai et al., 2003; Sakai et al., 2004; Sawada et al., 2002a; Sawada et al., 2002b). Its most widely documented role is that of assisting with sperm penetration through the ZP matrix. In this context, it has been shown that incubation of porcine, mouse and human sperm with exogenous proteasome inhibitors or anti-proteasome antibodies effectively blocks their ability to penetrate the ZP (Morales et al., 2003; Pasten et al., 2005; Sutovsky et al., 2004). Our preliminary examination of the proteasome in human spermatozoa supports these conclusions but also raises the possibility that it possesses an affinity for the ZP. Indeed, in our studies an antibody directed against representative 20S proteasome subunits (anti-'core') localized to the region responsible for interaction with the ZP and was able to significantly inhibit sperm binding to homologous zonae pellucidae. Similarly, labeling of the proteasome complex was detected on zonae pellucidae following incubation of oocytes with native sperm lysates. This binding was however virtually eliminated if the oocytes were pre-incubated with anti-ubiquitin antibodies to mask the ligands for proteasome adhesion.

In summary, this study has provided compelling evidence that human spermatozoa harbor a number of large membrane-bound protein complexes. Although the profile of these complexes is not dramatically influenced by the capacitation status of the sperm population, their relative levels of expression do show marked differences. The significance of these findings is highlighted by the identification of a sub-population of complexes that are both accessible to surface labeling techniques and that show affinity for homologous ZP. These results were validated by the characterization of two such complexes, each of which contained proteins that have been implicated in different aspects of sperm–ZP interaction. Collectively the mechanistic insights afforded by this study encourage a reassessment of models of sperm–ZP interactions, away from the simplistic 'lock-and-key' models that have dominated thinking for the past two decades. Characterization of the additional multiprotein complexes that were identified in the present study offers a number of exciting avenues for future research.

Acknowledgments

The authors are extremely grateful for the assistance of the staff and donors of the Hunter IVF clinic for the supply of oocytes to facilitate this study. This study was supported by grants from the National Health and Medical Research Council of Australia (NHMRC 569235) and Hunter Medical Research Institute (HMRI 08-15).

Appendix A. Supplementary data

Supplementary data to this article can be found online at doi:10.1016/j.ydbio.2011.05.674.

References

Alberts, B., 1998. The cell as a collection of protein machines: preparing the next generation of molecular biologists. Cell 92, 291–294.
Aquilina, J.A., Benesch, J.L., Ding, L.L., Yaron, O., Horwitz, J., Robinson, C.V., 2004. Phosphorylation of alphaB-crystallin alters chaperone function through loss of dimeric substructure. J. Biol. Chem. 279, 28675–28680.
Asquith, K.L., Baleato, R.M., McLaughlin, E.A., Nixon, B., Aitken, R.J., 2004. Tyrosine phosphorylation activates surface chaperones facilitating sperm-zona recognition. J. Cell Sci. 117, 3645–3657.
Austin, C.R., 1951. Observations on the penetration of the sperm in the mammalian egg. Aust. J. Sci. Res. B. 4, 581–596.
Aveldano, M.I., Rotstein, N.P., Vermouth, N.T., 1992. Lipid remodelling during epididymal maturation of rat spermatozoa. Enrichment in plasmenylcholines containing long-chain polyenoic fatty acids of the n−9 series. Biochem. J. 283 (Pt 1), 235–241.
Baker, M.A., Reeves, G., Hetherington, L., Muller, J., Baur, I., Aitken, R.J., 2007. Identification of gene products present in Triton X-100 soluble and insoluble fractions of human spermatozoa lysates using LC–MS/MS analysis. Proteomics Clin. Appl. 1, 524–532.
Biggers, J.D., Whitten, W.K., Whittingham, D.G., 1971. The culture of mouse embryos *in vitro*. In: Daniel, J.C.J. (Ed.), Methods in Mammalian Embryology. Freeman Press, San Francisco, CA, pp. 86–116.
Bose, S., Mason, G.G., Rivett, A.J., 1999. Phosphorylation of proteasomes in mammalian cells. Mol. Biol. Rep. 26, 11–14.
Camasses, A., Bogdanova, A., Shevchenko, A., Zachariae, W., 2003. The CCT chaperonin promotes activation of the anaphase-promoting complex through the generation of functional Cdc20. Mol. Cell. 12, 87–100.
Castano, J.G., Mahillo, E., Arizti, P., Arribas, J., 1996. Phosphorylation of C8 and C9 subunits of the multicatalytic proteinase by casein kinase II and identification of the C8 phosphorylation sites by direct mutagenesis. Biochemistry 35, 3782–3789.
Chang, M.C., 1951. Fertilizing capacity of spermatozoa deposited into the fallopian tubes. Nature 168, 697–698.
Cho, C., Bunch, D.O., Faure, J.E., Goulding, E.H., Eddy, E.M., Primakoff, P., Myles, D.G., 1998. Fertilization defects in sperm from mice lacking fertilin beta. Science 281, 1857–1859.
Cooper, T.G., 1986. The Epididymis, Sperm Maturation and Fertilisation. Springer-Verlag, Berlin.
Cornwall, G.A., 2009. New insights into epididymal biology and function. Hum. Reprod. Update 15, 213–227.
Cross, N.L., 2003. Decrease in order of human sperm lipids during capacitation. Biol. Reprod. 69, 529–534.
Ebnet, K., 2008. Organization of multiprotein complexes at cell–cell junctions. Histochem. Cell Biol. 130, 1–20.
Ecroyd, H., Meehan, S., Horwitz, J., Aquilina, J.A., Benesch, J.L., Robinson, C.V., Macphee, C.E., Carver, J.A., 2007. Mimicking phosphorylation of alphaB-crystallin affects its chaperone activity. Biochem. J. 401, 129–141.
Einspanier, R., Schuster, H., Schams, D., 1993. A comparison of hormone levels in follicle-lutein-cysts and in normal bovine ovarian follicles. Theriogenology 40, 181–188.
Ensslin, M.A., Shur, B.D., 2003. Identification of mouse sperm SED1, a bimotif EGF repeat and discoidin-domain protein involved in sperm–egg binding. Cell 114, 405–417.
Eubel, H., Braun, H.P., Millar, A.H., 2005. Blue-native PAGE in plants: a tool in analysis of protein–protein interactions. Plant Methods 1, 11.
Feldman, D.E., Thulasiraman, V., Ferreyra, R.G., Frydman, J., 1999. Formation of the VHL-elongin BC tumor suppressor complex is mediated by the chaperonin TRiC. Mol Cell. 4, 1051–1061.
Gadella, B.M., 2008. The assembly of a zona pellucida binding protein complex in sperm. Reprod. Domest. Anim. 43 (Suppl 5), 12–19.
Gadella, B.M., Tsai, P.S., Boerke, A., Brewis, I.A., 2008. Sperm head membrane reorganisation during capacitation. Int. J. Dev. Biol. 52, 473–480.
Gomez-Puertas, P., Martin-Benito, J., Carrascosa, J.L., Willison, K.R., Valpuesta, J.M., 2004. The substrate recognition mechanisms in chaperonins. J. Mol. Recognit. 17, 85–94.
Guenther, M.G., Yu, J., Kao, G.D., Yen, T.J., Lazar, M.A., 2002. Assembly of the SMRT-histone deacetylase 3 repression complex requires the TCP-1 ring complex. Genes Dev. 16, 3130–3135.
Harrison, R.A., Gadella, B.M., 2005. Bicarbonate-induced membrane processing in sperm capacitation. Theriogenology 63, 342–351.
Harrison, R.A., Ashworth, P.J., Miller, N.G., 1996. Bicarbonate/CO_2, an effector of capacitation, induces a rapid and reversible change in the lipid architecture of boar sperm plasma membranes. Mol. Reprod. Dev. 45, 378–391.
Hermo, L., Jacks, D., 2002. Nature's ingenuity: bypassing the classical secretory route *via* apocrine secretion. Mol. Reprod. Dev. 63, 394–410.
Heuberger, E.H., Veenhoff, L.M., Duurkens, R.H., Friesen, R.H., Poolman, B., 2002. Oligomeric state of membrane transport proteins analyzed with blue native electrophoresis and analytical ultracentrifugation. J. Mol. Biol. 317, 591–600.
Johnson, L.R., Pilder, S.H., Bailey, J.L., Olds-Clarke, P., 1995. Sperm from mice carrying one or two t haplotypes are deficient in investment and oocyte penetration. Dev. Biol. 168, 138–149.
Jones, R., 1989. Membrane remodelling during sperm maturation in the epididymis. Oxf. Rev. Reprod. Biol. 11, 285–337.
Jones, R., 1998. Plasma membrane structure and remodelling during sperm maturation in the epididymis. J. Reprod. Fertil. Suppl. 53, 73–84.
Katz, A., Waridel, P., Shevchenko, A., Pick, U., 2007. Salt-induced changes in the plasma membrane proteome of the halotolerant alga *Dunaliella salina* as revealed by blue native gel electrophoresis and nano-LC–MS/MS analysis. Mol. Cell. Proteomics 6, 1459–1472.

Kjell, J., Rasmusson, A.G., Larsson, H., Widell, S., 2004. Protein complexes of the plant plasma membrane resolved by Blue Native PAGE. Physiol. Plant. 121, 546–555.
Kubota, S., Kubota, H., Nagata, K., 2006. Cytosolic chaperonin protects folding intermediates of Gbeta from aggregation by recognizing hydrophobic beta-strands. Proc. Natl. Acad. Sci. U.S.A. 103, 8360–8365.
Leclerc, P., de Lamirande, E., Gagnon, C., 1996. Cyclic adenosine 3′,5′monophosphate-dependent regulation of protein tyrosine phosphorylation in relation to human sperm capacitation and motility. Biol. Reprod. 55, 684–692.
Leclerc, P., de Lamirande, E., Gagnon, C., 1998. Interaction between Ca^{2+}, cyclic 3′,5′ adenosine monophosphate, the superoxide anion, and tyrosine phosphorylation pathways in the regulation of human sperm capacitation. J. Androl. 19, 434–443.
Lefievre, L., Jha, K.N., de Lamirande, E., Visconti, P.E., Gagnon, C., 2002. Activation of protein kinase A during human sperm capacitation and acrosome reaction. J. Androl. 23, 709–716.
Leroux, M.R., Hartl, F.U., 2000. Protein folding: versatility of the cytosolic chaperonin TRiC/CCT. Curr. Biol. 10, R260–R264.
Lin, Y.N., Roy, A., Yan, W., Burns, K.H., Matzuk, M.M., 2007. Loss of zona pellucida binding proteins in the acrosomal matrix disrupts acrosome biogenesis and sperm morphogenesis. Mol. Cell. Biol. 27, 6794–6805.
Lippert, T.H., Seeger, H., Schieferstein, G., Voelter, W., 1993. Immunoreactive ubiquitin in human seminal plasma. J. Androl. 14, 130–131.
Lu, Q., Shur, B.D., 1997. Sperm from beta 1,4-galactosyltransferase-null mice are refractory to ZP3-induced acrosome reactions and penetrate the zona pellucida poorly. Development 124, 4121–4131.
Mason, G.G., Hendil, K.B., Rivett, A.J., 1996. Phosphorylation of proteasomes in mammalian cells. Identification of two phosphorylated subunits and the effect of phosphorylation on activity. Eur. J. Biochem. 238, 453–462.
Mitchell, L.A., Nixon, B., Aitken, R.J., 2007. Analysis of chaperone proteins associated with human spermatozoa during capacitation. Mol. Hum. Reprod. 13, 605–613.
Mitchell, L.A., Nixon, B., Baker, M.A., Aitken, R.J., 2008. Investigation of the role of SRC in capacitation-associated tyrosine phosphorylation of human spermatozoa. Mol. Hum. Reprod. 14, 235–243.
Morales, P., Cross, N.L., Overstreet, J.W., Hanson, F.W., 1989. Acrosome intact and acrosome-reacted human sperm can initiate binding to the zona pellucida. Dev. Biol. 133, 385–392.
Morales, P., Kong, M., Pizarro, E., Pasten, C., 2003. Participation of the sperm proteasome in human fertilization. Hum. Reprod. 18, 1010–1017.
Morales, P., Pizarro, E., Kong, M., Jara, M., 2004. Extracellular localization of proteasomes in human sperm. Mol. Reprod. Dev. 68, 115–124.
Mori, E., Baba, T., Iwamatsu, A., Mori, T., 1993. Purification and characterization of a 38-kDa protein, sp38, with zona pellucida-binding property from porcine epididymal sperm. Biochem. Biophys. Res. Commun. 196, 196–202.
Myles, D.G., Primakoff, P., 1984. Localized surface antigens of guinea pig sperm migrate to new regions prior to fertilization. J. Cell Biol. 99, 1634–1641.
Nijtmans, L.G., Henderson, N.S., Holt, I.J., 2002. Blue Native electrophoresis to study mitochondrial and other protein complexes. Methods 26, 327–334.
Nishimura, H., Cho, C., Branciforte, D.R., Myles, D.G., Primakoff, P., 2001. Analysis of loss of adhesive function in sperm lacking cyritestin or fertilin beta. Dev. Biol. 233, 204–213.
Nixon, B., Asquith, K.L., John Aitken, R., 2005. The role of molecular chaperones in mouse sperm-egg interactions. Mol. Cell. Endocrinol. 240, 1–10.
Nixon, B., MacIntyre, D.A., Mitchell, L.A., Gibbs, G.M., O'Bryan, M., Aitken, R.J., 2006. The identification of mouse sperm-surface-associated proteins and characterization of their ability to act as decapacitation factors. Biol. Reprod. 74, 275–287.
Nixon, B., Aitken, R.J., McLaughlin, E.A., 2007. New insights into the molecular mechanisms of sperm–egg interaction. Cell. Mol. Life Sci. 64, 1805–1823.
Nixon, B., Mitchell, L.A., Anderson, A., McLaughlin, E.A., O'Bryan, M., Aitken, R.J., in press. Proteomic and functional analysis of human sperm detergent resistant membranes. J Cell. Physiol. doi:10.1002/jcp.22615.
Olds-Clarke, P., Johnson, L.R., 1993. t haplotypes in the mouse compromise sperm flagellar function. Dev. Biol. 155, 14–25.
Olson, G.E., Hinton, B.T., 1985. Regional differences in luminal fluid polypeptides of the rat testis and epididymis revealed by two-dimensional gel electrophoresis. J. Androl. 6, 20–34.
Pasten, C., Morales, P., Kong, M., 2005. Role of the sperm proteasome during fertilization and gamete interaction in the mouse. Mol. Reprod. Dev. 71, 209–219.
Pilder, S.H., Lu, J., Han, Y., Hui, L., Samant, S.A., Olugbemiga, O.O., Meyers, K.W., Cheng, L., Vijayaraghavan, S., 2007. The molecular basis of "curlicue": a sperm motility abnormality linked to the sterility of t haplotype homozygous male mice. Soc. Reprod. Fertil. Suppl. 63, 123–133.
Sakai, N., Sawada, H., Yokosawa, H., 2003. Extracellular ubiquitin system implicated in fertilization of the ascidian, *Halocynthia roretzi*: isolation and characterization. Dev. Biol. 264, 299–307.
Sakai, N., Sawada, M.T., Sawada, H., 2004. Non-traditional roles of ubiquitin–proteasome system in fertilization and gametogenesis. Int. J. Biochem. Cell Biol. 36, 776–784.
Sali, A., Glaeser, R., Earnest, T., Baumeister, W., 2003. From words to literature in structural proteomics. Nature 422, 216–225.
Sawada, H., Sakai, N., Abe, Y., Tanaka, E., Takahashi, Y., Fujino, J., Kodama, E., Takizawa, S., Yokosawa, H., 2002a. Extracellular ubiquitination and proteasome-mediated degradation of the ascidian sperm receptor. Proc Natl Acad Sci U S A 99, 1223–1228.
Sawada, H., Takahashi, Y., Fujino, J., Flores, S.Y., Yokosawa, H., 2002b. Localization and roles in fertilization of sperm proteasomes in the ascidian *Halocynthia roretzi*. Mol. Reprod. Dev. 62, 271–276.
Schagger, H., von Jagow, G., 1991. Blue native electrophoresis for isolation of membrane protein complexes in enzymatically active form. Anal. Biochem. 199, 223–231.
Schagger, H., Cramer, W.A., von Jagow, G., 1994. Analysis of molecular masses and oligomeric states of protein complexes by blue native electrophoresis and isolation of membrane protein complexes by two-dimensional native electrophoresis. Anal. Biochem. 217, 220–230.
Shamsadin, R., Adham, I.M., Nayernia, K., Heinlein, U.A., Oberwinkler, H., Engel, W., 1999. Male mice deficient for germ-cell cyritestin are infertile. Biol. Reprod. 61, 1445–1451.
Shen, L., Weber, C.R., Turner, J.R., 2008. The tight junction protein complex undergoes rapid and continuous molecular remodeling at steady state. J Cell Biol. 181, 683–695.
Shotton, D.M., Burke, B.E., Branton, D., 1979. The molecular structure of human erythrocyte spectrin. Biophysical and electron microscopic studies. J. Mol. Biol. 131, 303–329.
Si, Y., Olds-Clarke, P., 1999. Mice carrying two t haplotypes: sperm populations with reduced Zona pellucida binding are deficient in capacitation. Biol. Reprod. 61, 305–311.
Silver, L.M., 1985. Mouse t haplotypes. Annu. Rev. Genet. 19, 179–208.
Silver, L.M., Artzt, K., Bennett, D., 1979. A major testicular cell protein specified by a mouse T/t complex gene. Cell 17, 275–284.
Soues, S., Kann, M.L., Fouquet, J.P., Melki, R., 2003. The cytosolic chaperonin CCT associates to cytoplasmic microtubular structures during mammalian spermiogenesis and to heterochromatin in germline and somatic cells. Exp. Cell Res. 288, 363–373.
Sternlicht, H., Farr, G.W., Sternlicht, M.L., Driscoll, J.K., Willison, K., Yaffe, M.B., 1993. The t-complex polypeptide 1 complex is a chaperonin for tubulin and actin *in vivo*. Proc Natl Acad Sci U S A 90, 9422–9426.
Sutovsky, P., Moreno, R., Ramalho-Santos, J., Dominko, T., Thompson, W.E., Schatten, G., 2001. A putative, ubiquitin-dependent mechanism for the recognition and elimination of defective spermatozoa in the mammalian epididymis. J Cell Sci. 114, 1665–1675.
Sutovsky, P., Manandhar, G., McCauley, T.C., Caamano, J.N., Sutovsky, M., Thompson, W.E., Day, B.N., 2004. Proteasomal interference prevents zona pellucida penetration and fertilization in mammals. Biol. Reprod. 71, 1625–1637.
Syntin, P., Dacheux, F., Druart, X., Gatti, J.L., Okamura, N., Dacheux, J.L., 1996. Characterization and identification of proteins secreted in the various regions of the adult boar epididymis. Biol. Reprod. 55, 956–974.
Takakuwa, Y., Tchernia, G., Rossi, M., Benabadji, M., Mohandas, N., 1986. Restoration of normal membrane stability to unstable protein 4.1-deficient erythrocyte membranes by incorporation of purified protein 4.1. J. Clin. Invest. 78, 80–85.
Thériault, J.R., Lambert, H., Chávez-Zobel, A.T., Charest, G., Lavigne, P., Landry, J., 2004. Essential role of the NH2-terminal WD/EPF motif in the phosphorylation-activated protective function of mammalian Hsp27. J. Biol. Chem. 28, 23463–23471.
Towbin, H., Staehelin, T., Gordon, J., 1979. Electrophoretic transfer of proteins from polyacrylamide gels to nitrocellulose sheets: procedure and some applications. Proc Natl Acad Sci U S A 76, 4350–4354.
Visconti, P.E., Bailey, J.L., Moore, G.D., Pan, D., Olds-Clarke, P., Kopf, G.S., 1995a. Capacitation of mouse spermatozoa. I. Correlation between the capacitation state and protein tyrosine phosphorylation. Development 121, 1129–1137.
Visconti, P.E., Moore, G.D., Bailey, J.L., Leclerc, P., Connors, S.A., Pan, D., Olds-Clarke, P., Kopf, G.S., 1995b. Capacitation of mouse spermatozoa. II. Protein tyrosine phosphorylation and capacitation are regulated by a cAMP-dependent pathway. Development 121, 1139–1150.
Ward, W.S., Zalensky, A.O., 1996. The unique, complex organization of the transcriptionally silent sperm chromatin. Crit. Rev. Eukaryot. Gene Expr. 6, 139–147.
Wehren, A., Meyer, H.E., Sobek, A., Kloetzel, P.M., Dahlmann, B., 1996. Phosphoamino acids in proteasome subunits. Biol. Chem. 377, 497–503.
Wittig, I., Braun, H.P., Schagger, H., 2006. Blue native PAGE. Nat. Protoc. 1, 418–428.
Won, K.A., Schumacher, R.J., Farr, G.W., Horwich, A.L., Reed, S.I., 1998. Maturation of human cyclin E requires the function of eukaryotic chaperonin CCT. Mol. Cell. Biol. 18, 7584–7589.
Yanagimachi, R., 1994. Fertility of mammalian spermatozoa: its development and relativity. Zygote 2, 371–372.
Yanagimachi, R., Lopata, A., Odom, C.B., Bronson, R.A., Mahi, C.A., Nicolson, G., 1979. Retention of biologic characteristics of zona pellucida in highly concentrated salt solution: the use of salt stored eggs for assessing the fertilizing capacity of spermatozoa. Fertil. Steril. 31, 471–476.